



K. N. Toosi University of Technology  
Faculty of Electrical and Computer Engineering

## **Robust Control of Automatic Voltage Regulator (AVR)**

By:

**Vahe Karimian**

Course Instructor:

**Dr.Mahsan Tavakoli Kakhki**

Summer 2024

# Table of Contexts

page

<b>Abstract .....</b>	<b>3</b>
<b>Section 1: Introducing dynamic system .....</b>	<b>4</b>
<b>Section 2: <math>\mu</math>-synthesis control design .....</b>	<b>8</b>
<b>Section 3: <math>H^\infty</math> control design (RICC &amp; LMI) .....</b>	<b>22</b>
<b>Section 4: <math>H_2</math> control design .....</b>	<b>41</b>
<b>Section 5: <math>H_2/H^\infty</math> control design .....</b>	<b>48</b>
<b>Section 6: Parameteric controller design .....</b>	<b>56</b>
<b>Conclusion .....</b>	<b>62</b>
<b>References .....</b>	<b>63</b>
<b>Appendix .....</b>	<b>64</b>

## Abstract

In this study, novel controllers utilizing  $H_\infty$  and structured singular value decomposition has been introduced to enhance the robustness of the Automatic Voltage Regulator (AVR) system. The controller accounts for six distinct uncertainties in the actuator, exciter, and generator, which manifest as variations in linear transfer functions due to load fluctuations and aging effects over time. The effectiveness of this approach hinges on two key factors. Firstly, it simultaneously addresses output disturbances, sensor noise, and system uncertainties during the controller design process. Secondly, it incorporates a non-conservative modeling approach for all six structured parameters within the required  $\mu$ -synthesis  $P-\Delta-K$  configuration. Through suboptimal  $H_\infty$  control design and  $\mu$ -analysis theorem and  $\mu$ -synthesis control design, a single-input, single-output (SISO) controller is derived, resulting in a closed-loop system where  $\mu < 1$  is achieved.

## Section 1: Introducing Dynamic System

In the operation of a synchronous generator, the terminal voltage is monitored against a reference value. The automatic voltage regulator (AVR) adjusts the generator's field voltage based on this error signal to manage the reactive power supplied to the load. Additionally, the AVR's primary role is to maintain the terminal voltage magnitude of the synchronous generator at a specified level.

However, due to various complexities in power system performance, such as nonlinear characteristics, fluctuating loads, varying operating conditions, and the significant inductance of generator field windings, achieving a rapid and stable response from the regulator poses challenges. Therefore, enhancing the AVR's performance, robustness, and speed is crucial. This improvement can be achieved by employing a controller to ensure the closed-loop system efficiently responds to sudden changes in terminal voltage.

The parameters of the AVR's linear time-invariant (LTI) model fluctuate significantly with various operating conditions. Consequently, a controller designed solely for the nominal operating point of the AVR system may not ensure robust performance. Therefore, there has always been a necessity to design a controller that can enhance the robustness of the AVR system. However, why is the  $\mu$ -theorem necessary for controlling the AVR system? This question is crucial.

Developing a controller for the AVR system using linear control methods necessitates using a nominal LTI power system model derived from a specific operating state. This model captures the dynamic behavior of the power system

around the mentioned operating condition, with parameters having real values that range between their minimum and maximum bounds. Given that these parameters represent structured uncertainties, employing  $H_\infty$  and  $\mu$ -synthesis is suitable for enhancing the robustness of the AVR system, and the  $\mu$ -theorem provides a direct method to analyze its robust performance.

A basic AVR system comprises four primary subsystems: amplifier, generator, sensor, and exciter. Each of these blocks can be represented in a simple linear transfer function (LTF) form, typically as a first-order LTF characterized by a time constant and a gain. By treating minor variations in the gain and time constant of the sensor transfer function as negligible, they are excluded from the set of uncertainties. Consequently, the AVR system is left with six real structured uncertainties: the time and gain constants of the amplifier, exciter, and synchronous generator.

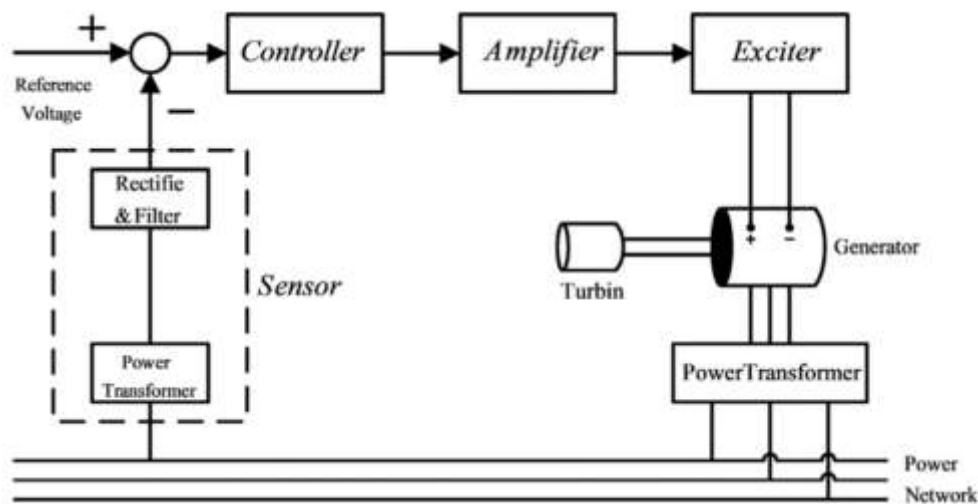


**Fig. 1:** The schematic diagram of a typical single-machine infinite-bus system

Figure 1 illustrates the schematic diagram of a standard Single Machine Infinite Bus (SMIB) power generation system. This system comprises a synchronous

generator connected to an infinite bus. In the electrical section, there are two primary control loops: Automatic Voltage Regulator (AVR) and Automatic Load-Frequency Control (ALFC), along with a supplementary controller called Power System Stabilizer (PSS) to automatically adjust the local voltage terminal and load frequency. The generator's shaft frequency is monitored, and a governor regulates the mechanical power and rotor speed based on turbine feedback.

Precisely controlling the excitation voltage of the synchronous generator is crucial for enhancing power system stability and performance. The AVR adjusts the generator's excitation voltage to maintain its output voltage at a specific level.

**Table 1**  
Transfer function of AVR components.

Component	Transfer function	Gain limit	Time constant limit
Amplifier	$G_A = \frac{K_A}{T_A s + 1}$	$10 \leq K_A \leq 40$	$0.02 \text{ s} \leq T_A \leq 0.1 \text{ s}$
Exciter	$G_E = \frac{K_E}{T_E s + 1}$	$1 \leq K_E \leq 10$	$0.4 \text{ s} \leq T_E \leq 1 \text{ s}$
Generator	$G_G = \frac{K_G}{T_G s + 1}$	$0.7 \leq K_G \leq 1$	$1 \text{ s} \leq T_G \leq 2 \text{ s}$
Forward transfer function	$G_F = G_A G_E G_G = \frac{K_F}{(T_A s + 1)(T_E s + 1)(T_G s + 1)}$		$7 \leq K_F \leq 400$
Sensor	$G_S = \frac{K_S}{T_S s + 1}$	$K_S = 1$	$T_S = 0.006 \text{ s}$

In its basic configuration, each component of the AVR system—exciter, amplifier, sensor, and generator—can be represented by a first-order transfer function characterized by a time constant and gain. These parameters can vary due to load fluctuations, changes in operating conditions, and deviations in system parameters, as detailed in Table 1.

The block diagram of the AVR system in Figure 1 consists of five distinct blocks, as depicted in Figure 2.

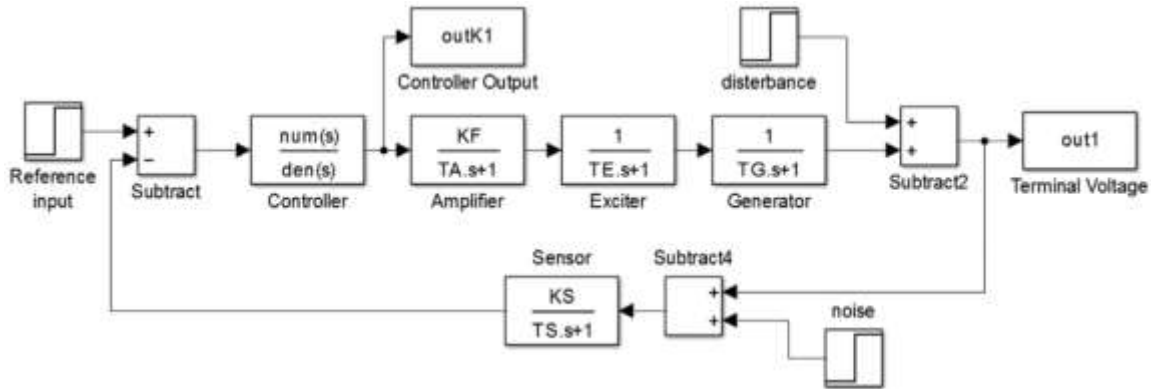


**Fig. 2:**The block diagram of the AVR system

The  $\mu$  (Singular Value Decomposition) theorem was introduced by J. Doyle in 1982 and serves as a powerful tool for analyzing and designing robust control systems that deal with real structured uncertainties. The primary objectives of employing H infinity and  $\mu$  theorems include treating system parameters as real parametric uncertainties, constraining the controller's output, and directly modeling output disturbances and noise. These objectives stem from critical considerations such as achieving a single-input, single-output (SISO) system, ensuring minimum phase and minimum degree linear controllers that offer robust performance. These controllers can be seamlessly integrated at minimal cost, replacing industrial voltage controllers without necessitating changes to the AVR system, sensor types, or actuator structures.

In the future, this introduced linear robust controller can serve as a reference point for studying the performance of other robust controllers designed through various approaches, whether linear (such as loop-shaping and quantitative feedback theory) or nonlinear methods like disturbance observer techniques to compensate for uncertainties.

## Section 2: $\mu$ -synthesis control design

To analyze and design a controller for a model with uncertainties, the diagram in Fig. 3 is proposed. In Fig. 3,  $u$  represents external inputs to the system such as disturbances, commands, and noise. The output  $e$  typically includes system output, filtered signals, and tracking errors.  $P_o$  and  $P_i$  denote the output and input signals of the uncertainties, respectively. Feedback signals  $y$  are inputs to the controller, and  $C$  indicates the control signals from the controller.  $P$  represents the nominal open-loop interconnected transfer function matrix, excluding the controller  $K$ , uncertainties, and perturbations. The robust stability (RS) and robust performance (RP) of the system can be expressed as:

- Robust performance: (RP)  $\Leftrightarrow \mu_{\tilde{\Delta}}(M) < 1$  for mixed structured and unstructured uncertainty  $\tilde{\Delta}$ .
- Robust stability: (RS)  $\Leftrightarrow \mu_{\Delta}(M_{11}) < 1$  for structured uncertainty  $\Delta$ .
- Nominal performance: (NP)  $\Leftrightarrow \|M_{22}\|_{\infty} < 1$ .
- Nominal stability: (NS)  $\Leftrightarrow M$  is internally stable.

By the unstructured uncertainty  $\Delta$ , the robust stability requirement equals to  $\|M_{11}\|_{\infty} < 1$ . Also, for the robust stability robust performance (RSRP) design, finding a controller  $K$  is necessary that:

$$\sup_{\mu_{\tilde{\Delta}}} [M(P, K)(j\omega)] < 1 \quad \omega \in \mathbb{R}$$



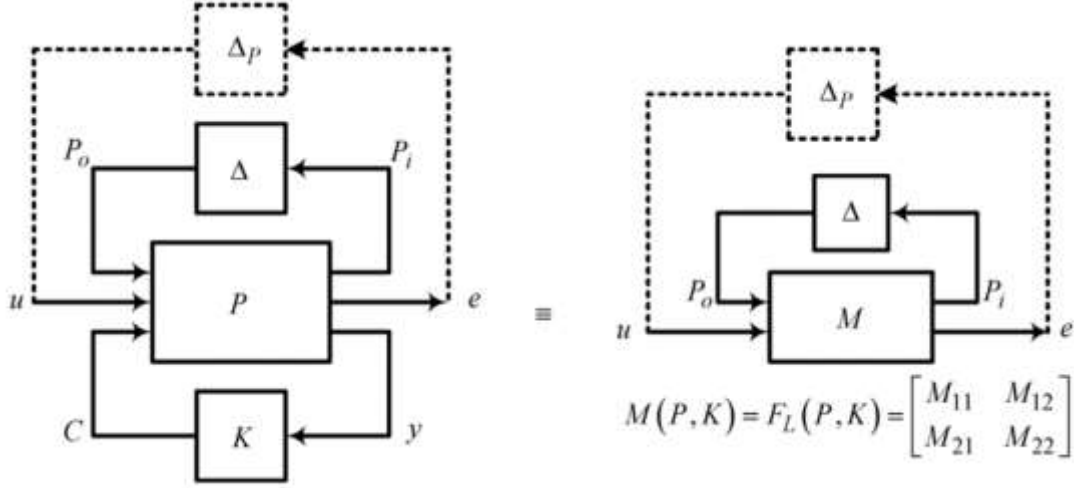


Fig. 3: P-Δ-K representation of robust control system

An input multiplicative uncertainty is considered (Fig. 4). Fig. 5 shows the system closed-loop in the presence of the structured diagonal uncertainty and weighting functions blocks.

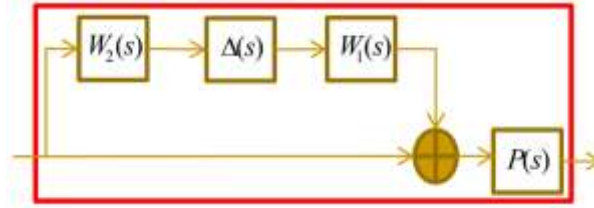


Fig. 4: Uncertain system with input multiplicative uncertainty

As shown in Fig. 6 the upper bound function of uncertainty ( $W$ ) is obtained by changing values of uncertain parameters and using following relation( $W_2=I$ ):

$$\left| \frac{\Pi}{P_0} - 1 \right| < |W(j\omega)| \quad (1)$$

Here,  $\Pi$  represents the uncertain system model and  $P_0$  is the nominal system model( $\Pi = P_0(1+\Delta W)$ ).  $P_0$  is considered by mean values of uncertain parameters:

$$P_0 = \frac{203.5}{(0.06s+1)(0.7s+1)(1.5s+1)}$$

$P_0$  is stable having three poles in -16.67, -1.43 and -0.67.

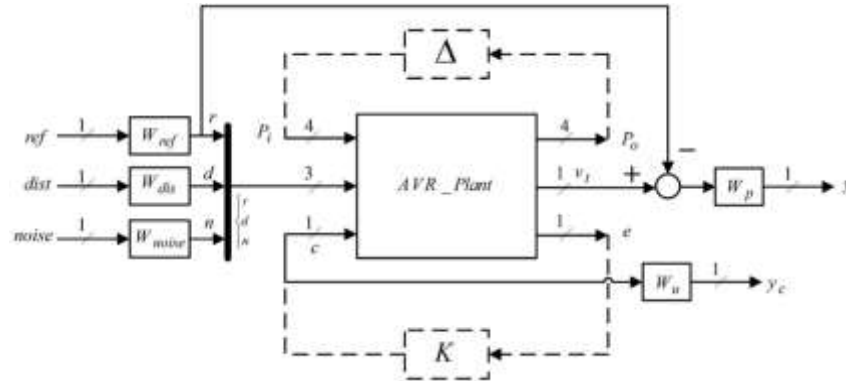


**Fig. 5:** Closed-loop system in the presence of structured uncertainty and weighting function blocks

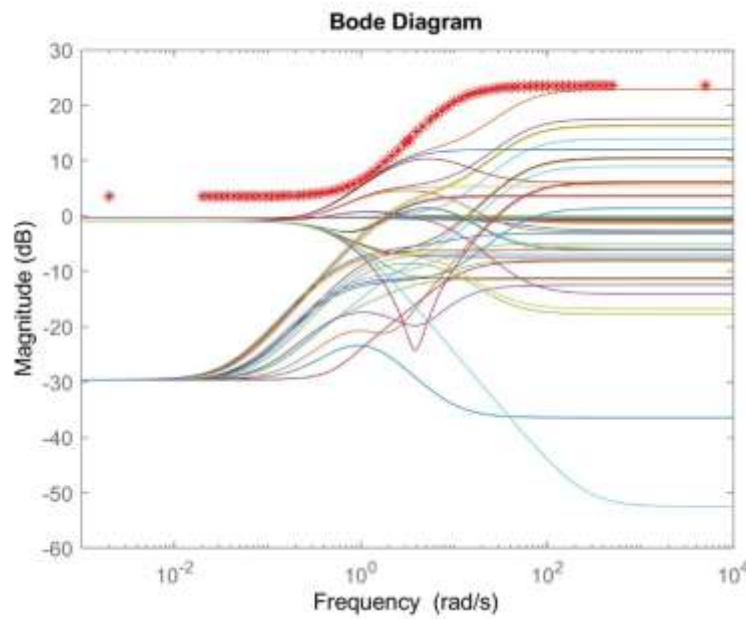


**Fig. 6:** Bode magnitude diagram of relation (1)

In Fig. 6 the Bode diagram of  $W$  is shown with red stars and obtained as following:

$$W = 15 \frac{s+1}{s+10}$$

$W_p$  is the performance weighting function for the output voltage of the generator and bounds the system's sensitivity function ( $S(s) \leq W_p^{-1}(s)$ ) to create the possible small sensitivity output disturbances as:

$$W_p(s) = \frac{s+220}{210000s+1}$$

On the other hand, for confining the control system energy, the control weighting functions ( $W_u$ ) have been selected to decrease the magnitude of the controller outputs. The following structure has been chosen for  $W_u$ .

$$W_u(s) = \frac{0.1s+2}{s+20}$$

Fig. 7 and Fig. 8 shows the magnitude curve of the reverse of the performance function ( $W_p^{-1}$ ) and control weighting function ( $W_u$ ).

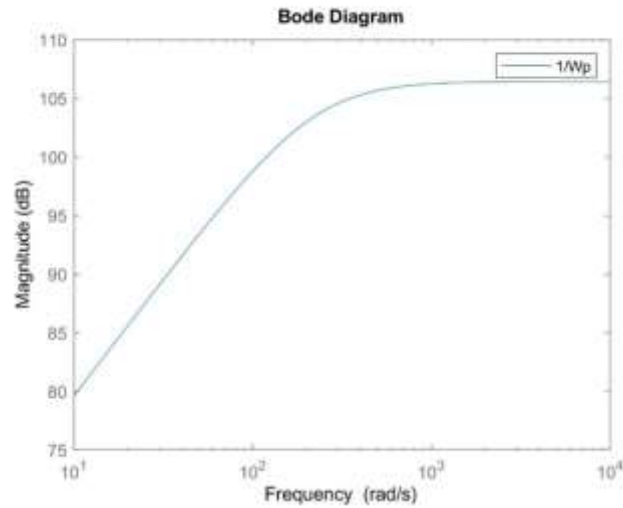


**Fig. 7:** Bode magnitude plot of inverse of the performance weighting function

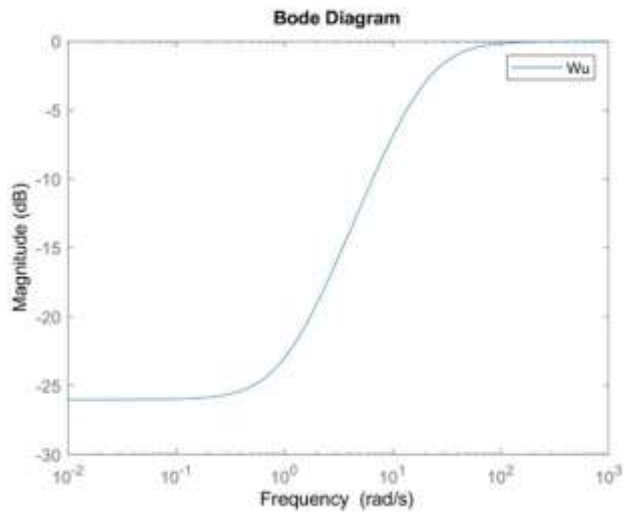


**Fig. 8:** Bode magnitude plot of the control weighting function

After introducing interconnected system for the uncertain plant, D-K iteration method is used to sketch the suboptimal  $\mu$ -synthesis controller by a Matlab appropriate code. By defining the  $\tilde{\Delta}$  block as (2), the robust performance (RP) of the designed system is obtained, if and only if  $\mu_{\tilde{\Delta}}(\cdot) < 1$  for each frequency.

$$\tilde{\Delta} := \left\{ \begin{bmatrix} \Delta & 0 \\ 0 & \Delta_p \end{bmatrix} : \Delta \in R^{4 \times 4}, \Delta_p \in C^{3 \times 2} \right\} \quad (2)$$

Fig. 9 shows the upper linear fractional of the closed loop system by existing the structured and unstructured uncertainties ( $F_U (AVR\_ic, \tilde{\Delta})$ ).

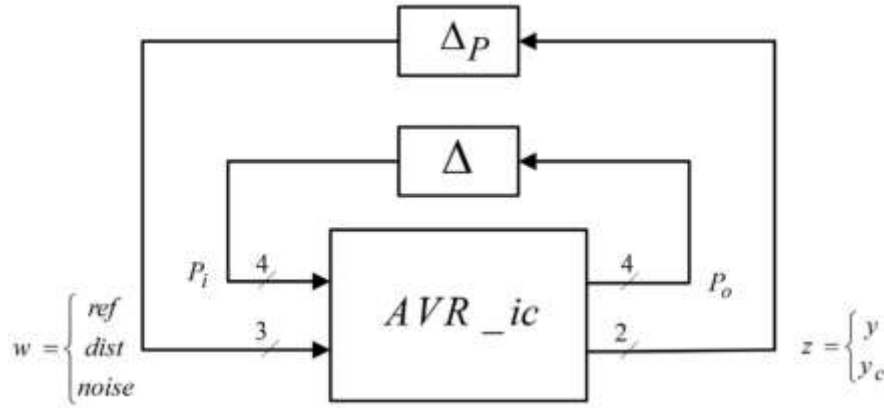


Fig. 9: Upper linear fractional of the closed loop system in the presence of the structured and unstructured uncertainties

On the basis of the above procedure and the data of Table 1, a seven order SISO controller has been obtained like as Eq.(3) where its  $\mu$  value is less than one. The bode diagram of this appropriate controller is represented in Fig. 10.

$$\mathbf{K}(s) = \frac{0.019s^6 + 41.14s^5 + 1706s^4 + 2.641e4s^3 + 1.566e5s^2 + 2.496e5s + 1.065e5}{s^7 + 361.8s^6 + 2.349e4s^5 + 7.302e5s^4 + 1.256e7s^3 + 9.092e7s^2 + 9.539e7s + 454.3} \quad (3)$$

The controller design has done in three iterations. Fig. 11 depicts the  $\mu$  plot of closed-loop system on each iteration.

In this section, some scenarios have been considered to show the merit of the robust performance of the designed controller. These scenarios have been adopted based on the nominal values, maximum values, minimum values and the tolerance percentages of the system uncertainties by existing the output disturbance.

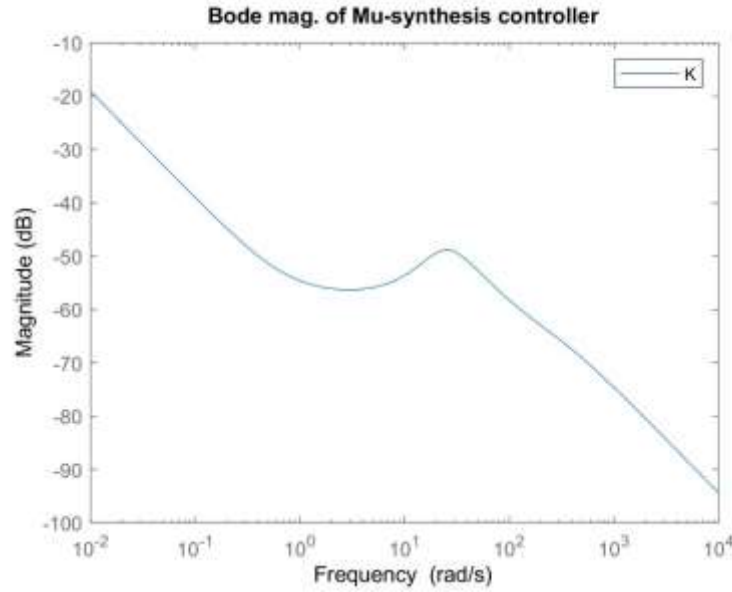


**Fig. 10:** Bode magnitude diagram of  $\mu$ -synthesis controller

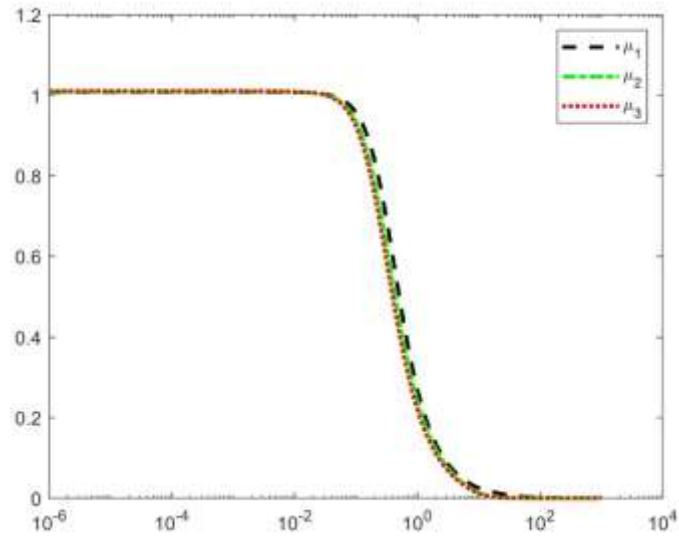


**Fig. 11:** Closed loop  $\mu$  plot on each iteration

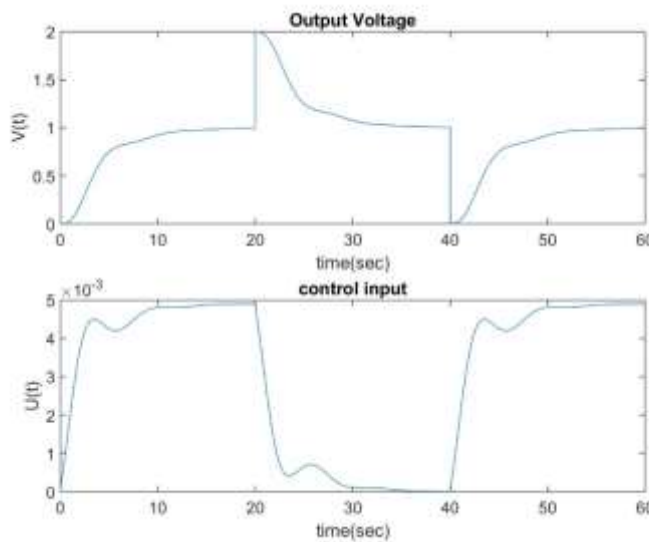
In all simulations, this pattern has been considered to assess the controllers' performance:

1. There is a  $1^{pu}$  change in the reference voltage at  $t = 0$  for analyzing the tracking performance.
2. In order to analyze short circuit faults, the generator's terminal voltage will be zero by a  $-1^{pu}$  sudden disturbance at the output terminal voltage. In this case, the controllers must return the output voltage to the reference value.
3. By a sudden increment in the terminal voltage to  $2^{pu}$ , the transient overvoltage can be modeled. For this modeling a  $1^{pu}$  voltage disturbance has been added to the terminal voltage.

These patterns are applied to the AVR system in three points of functional area according to the following five scenarios:

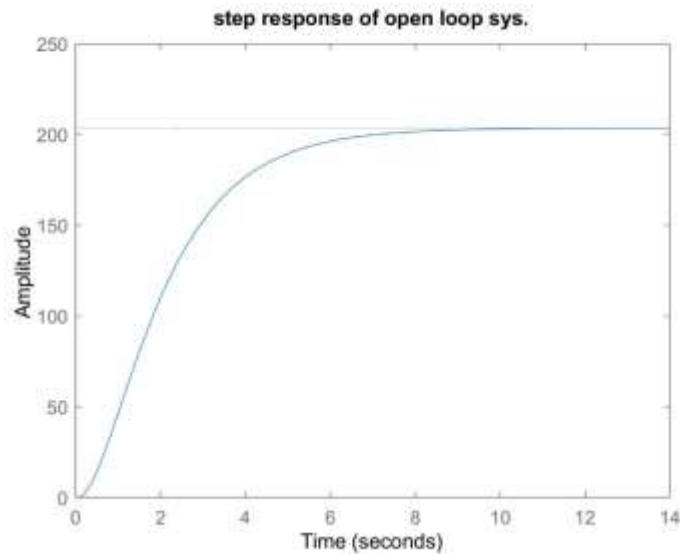
- 1– The nominal values of time constants and gains of the transfer functions.
- 2– The maximum values of time constants and gains of the transfer functions.
- 3– The minimum values of time constants and gains of the transfer functions.

**Scenario 1:**  $K_F=203.5$  ,  $T_A=0.06$  ,  $T_E=0.7$  ,  $T_G=1.5$

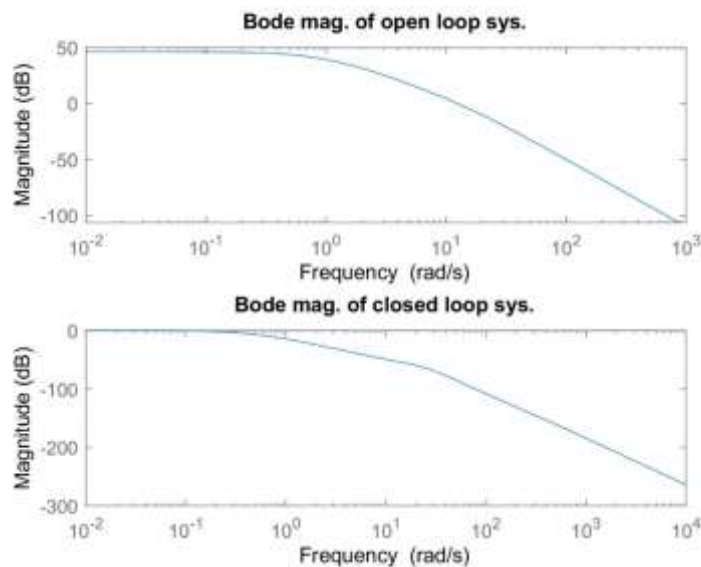


**Fig. 12:** Output voltage and control input plot for scenario 1

Fig. 12 depicts step response of closed loop system. Fig. 13 depicts step response of open loop system and Fig. 14 depicts bode magnitude diagrams of open loop and closed loop systems.

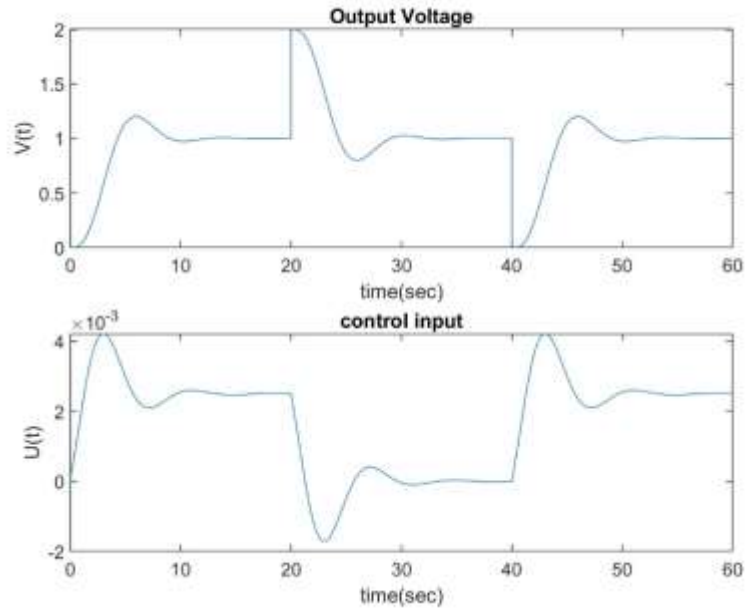


**Fig. 13:** Step response of open loop system



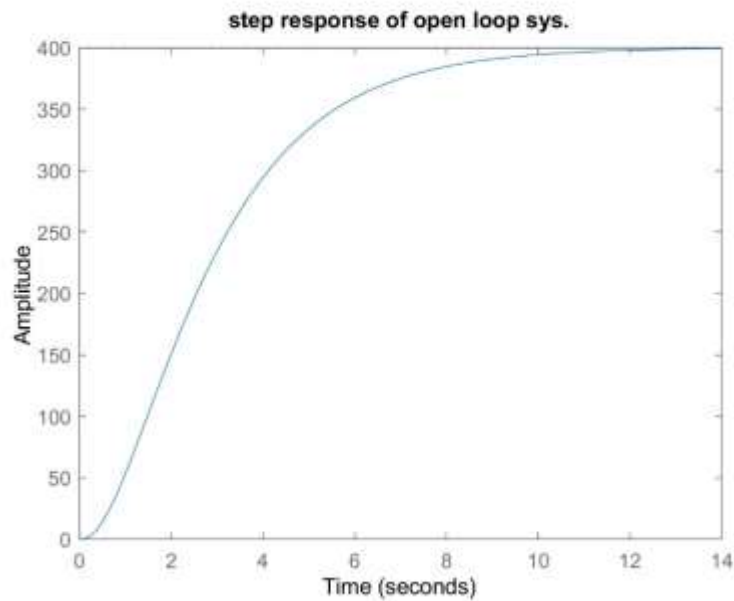
**Fig. 14:** Bode magnitude diagram of open loop and closed loop systems

**Scenario 2:**  $KF=400$  ,  $TA=0.1$  ,  $TE=1$  ,  $TG=2$



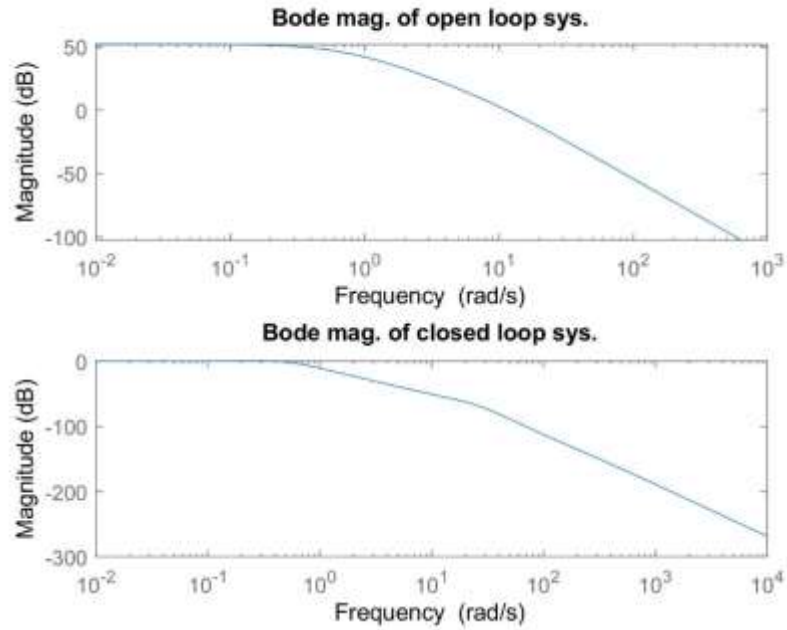
**Fig. 15:** Output voltage and control input plot for scenario 2

Fig. 15 depicts step response of closed loop system. Fig. 16 depicts step response of open loop system and Fig. 17 depicts bode magnitude diagrams of open loop and closed loop systems.



**Fig. 16:** Step response of open loop system





**Fig. 17:** Bode magnitude diagram of open loop and closed loop systems

**Scenario 3:**  $K_F=7$  ,  $T_A=0.02$  ,  $T_E=0.4$  ,  $T_G=1$

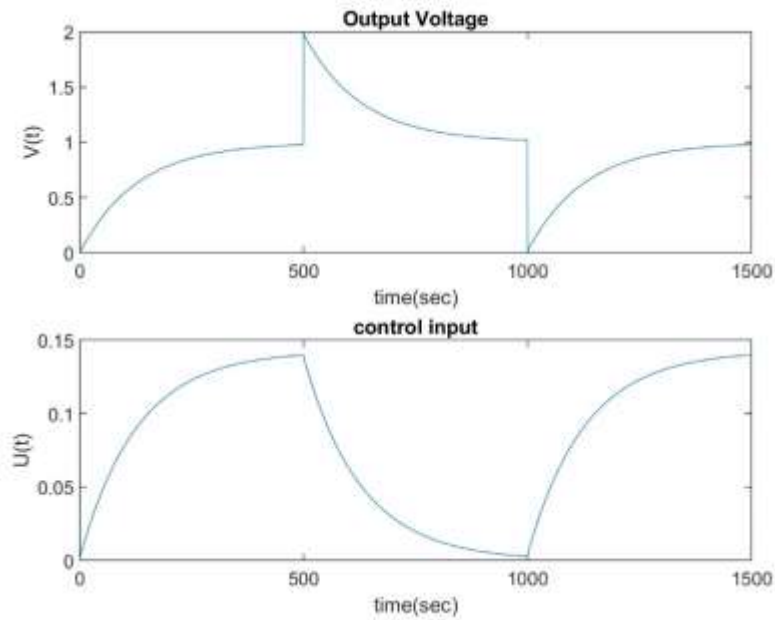


**Fig. 18:** Output voltage and control input plot for scenario 3

Fig. 18 depicts step response of closed loop system. Fig. 19 depicts step response of open loop system and Fig. 20 depicts bode magnitude diagrams of open loop and closed loop systems.

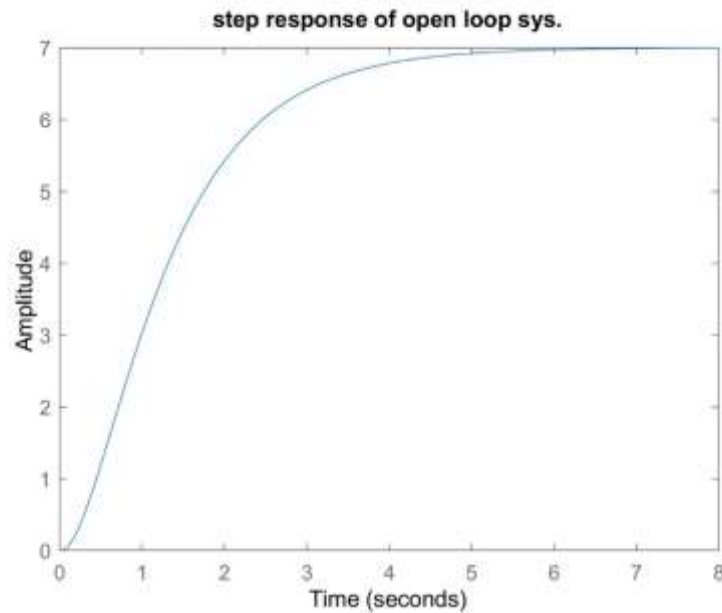


**Fig. 19:** Step response of open loop system

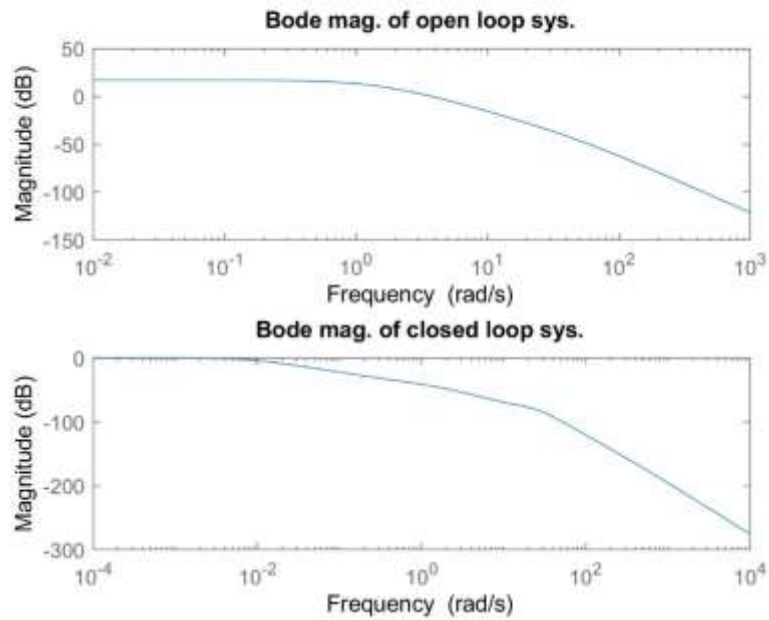


**Fig. 20:** Bode magnitude diagram of open loop and closed loop systems

If the nominal values and tolerance percentages of these uncertainties have been conveyed by  $(\tilde{K}_F, P_{KF})$  and  $(\tilde{T}_i, P_{Ti})$  respectively, the uncertainties in the structure of upper linear fractional transforming (LFT) can be demonstrated by:

$$\tilde{K}_F = \frac{KF(\min) + KF(\max)}{2} \quad P_{KF} = \frac{KF(\max) - KF(\min)}{KF(\max) + KF(\min)} \quad (4)$$

$$\tilde{T}_i = \frac{Ti(\min) + Ti(\max)}{2} \quad P_{Ti} = \frac{Ti(\max) - Ti(\min)}{Ti(\max) + Ti(\min)} \quad (5)$$

$$K_F = \tilde{K}_F(1 + \delta_{KF} P_{KF}) \quad , \quad \delta_{KF} \in [-1 \ 1] \quad (6)$$

$$\frac{1}{T_i} = \frac{1}{\tilde{T}_i} - \frac{P_{Ti}}{\tilde{T}_i} \delta_{Ti} (1 + \delta_{Ti} P_{Ti})^{-1} \quad (7)$$

The block diagram of a first order transfer function  $(\frac{K_F}{1+T_i s})$  with LFTs block diagram of its uncertainties  $(K_F, T_i)$  has been demonstrated in Fig. 21.

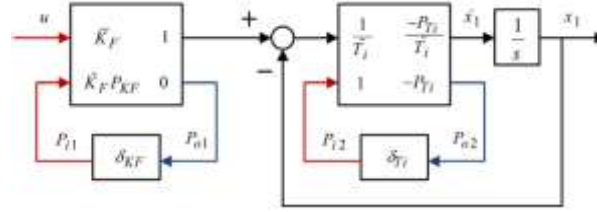


**Fig. 21:** Block diagram for P-D representation of the  $K_F/(1+T_i s)$  transfer function with  $K_F$  and  $T_i$  uncertainties

Here, in Eq. (8) the state space representation of interconnected system in presence of weighting matrices has been introduced. one can use this matrix to calculate structured singular value of uncertain closed loop system.

$$\begin{bmatrix} \dot{x}_1 \\ \dot{x}_2 \\ \dot{x}_3 \\ \dot{x}_4 \\ \dot{x}_5 \\ \dot{x}_6 \\ p_{01} \\ p_{02} \\ p_{03} \\ p_{04} \\ z_p \\ z_u \\ e \end{bmatrix} = \begin{bmatrix} \frac{-1}{\tilde{T}_A} & 0 & 0 & 0 & 0 & 0 & \frac{1}{\tilde{T}_A} & \frac{-P_{TA}}{\tilde{T}_A} & 0 & 0 & 0 & 0 & 0 & \frac{\tilde{K}_F}{\tilde{T}_A} \\ \frac{1}{\tilde{T}_E} & \frac{-1}{\tilde{T}_E} & 0 & 0 & 0 & 0 & 0 & 0 & \frac{-P_{TE}}{\tilde{T}_G} & 0 & 0 & 0 & 0 & 0 \\ 0 & \frac{1}{\tilde{T}_G} & \frac{-1}{\tilde{T}_G} & 0 & 0 & 0 & 0 & 0 & 0 & \frac{-P_{TG}}{\tilde{T}_G} & 0 & 0 & 0 & 0 \\ 0 & 0 & \frac{K_S}{\tilde{T}_S} & \frac{-1}{\tilde{T}_S} & 0 & 0 & 0 & 0 & 0 & 0 & \frac{K_S}{\tilde{T}_S} & \frac{K_S}{\tilde{T}_S} & 0 & 0 \\ 0 & 0 & 0 & -10.48 & 4.8e-6 & 0 & 0 & 0 & 0 & 0 & 10.48 & 0 & 0 & 0 \\ 0 & 0 & 0 & 0 & 0 & 20 & 0 & 0 & 0 & 0 & 0 & 0 & 0 & -19 \\ 0 & 0 & 0 & 0 & 0 & 0 & 0 & 0 & 0 & 0 & 0 & 0 & 0 & \tilde{K}_F P_{KF} \\ -1 & 0 & 0 & 0 & 0 & 0 & 0 & 0 & -P_{TA} & 0 & 0 & 0 & 0 & \tilde{K}_F \\ 1 & -1 & 0 & 0 & 0 & 0 & 0 & 0 & 0 & -P_{TA} & 0 & 0 & 0 & 0 \\ 0 & 1 & -1 & 0 & 0 & 0 & 0 & 0 & 0 & 0 & -P_{TG} & 0 & 0 & 0 \\ 0 & 0 & 0 & -4.76 & 1 & 0 & 0 & 0 & 0 & 0 & 0 & 4.76 & 0 & 0 \\ 0 & 0 & 0 & 0 & 0 & 1 & 0 & 0 & 0 & 0 & 0 & 0 & 0 & 1 \\ 0 & 0 & 0 & -1 & 0 & 0 & 0 & 0 & 0 & 0 & 0 & 1 & 0 & 0 \end{bmatrix} \begin{bmatrix} x_1 \\ x_2 \\ x_3 \\ x_4 \\ x_5 \\ x_6 \\ p_{i1} \\ p_{i2} \\ p_{i3} \\ p_{i4} \\ p_{i5} \\ r \\ d \\ n \\ u \end{bmatrix} \quad (8)$$

## Simulation a real synchronous generator connected to a 230 kV network

Here, a 200 MVA, 13.8 kV, 112.5 rpm generator has been studied which is linked to a 230 kV network via a Delta-Y 210 MVA transformer(Fig. 24). The system initiates in steady state with the generator supplying 150 MW of active power. At  $t = 0.1$  s, a three-phase to ground fault occurs on the 230 kV bus of the transformer. The fault is cleared followed by 6 cycles. The synchronous generator has been modeled by 7-order nonlinear equations and has a separated LFC control system (governor, turbine, and PID frequency controller). To apply our designed robust controller, its transfer function equation with the amplifier and exciter has been substituted instead of the original AVR controller without any change in the system structure and parameters. Fig. 22 and 23 represent the deviation of the voltage terminal magnitude by the controller. Although our controller has not been designed strictly for this system, its performance is obviously acceptable. If the synchronous generator parameters have been considered and the gain and time constant of its 1-order model computed, the controller could be designed perfectly for this system.

**Scenario 1:**  $K_A=40$  ,  $K_E=10$  (maximum)

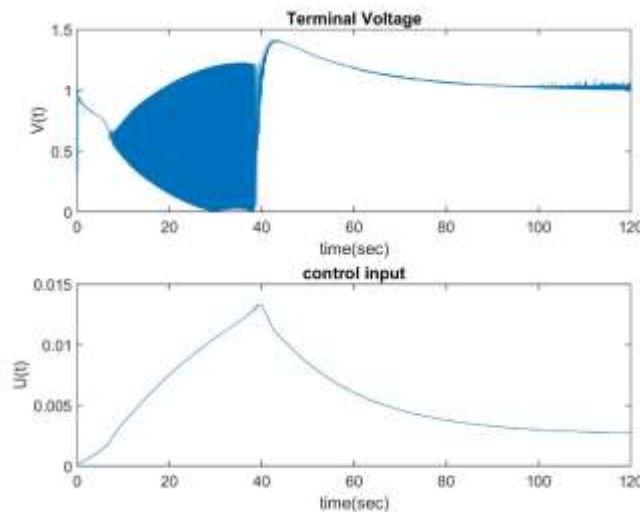


**Fig. 22:** Terminal voltage and control input for scenario 1

**Scenario 2:**  $KA=10$  ,  $KE=1$  (minimum)

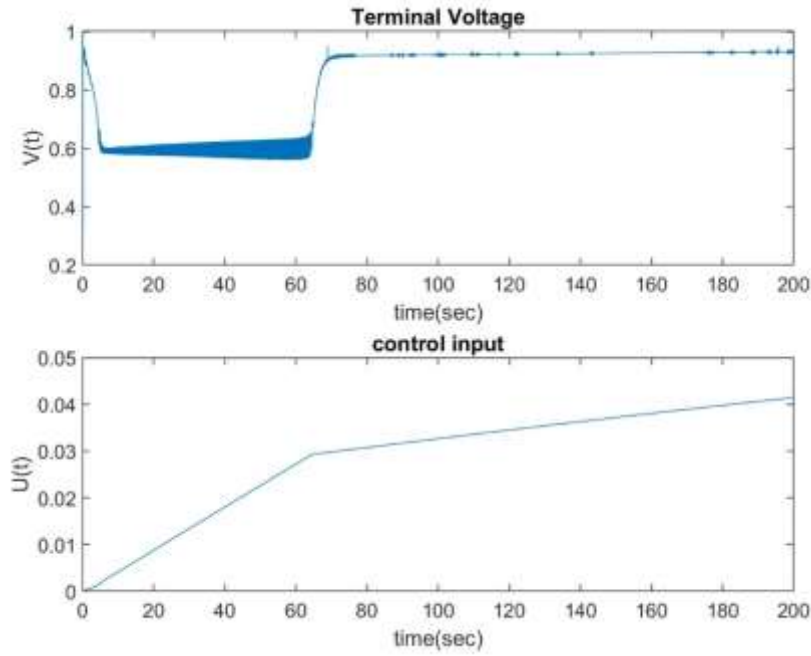


**Fig. 23:** Terminal voltage and control input for scenario 2

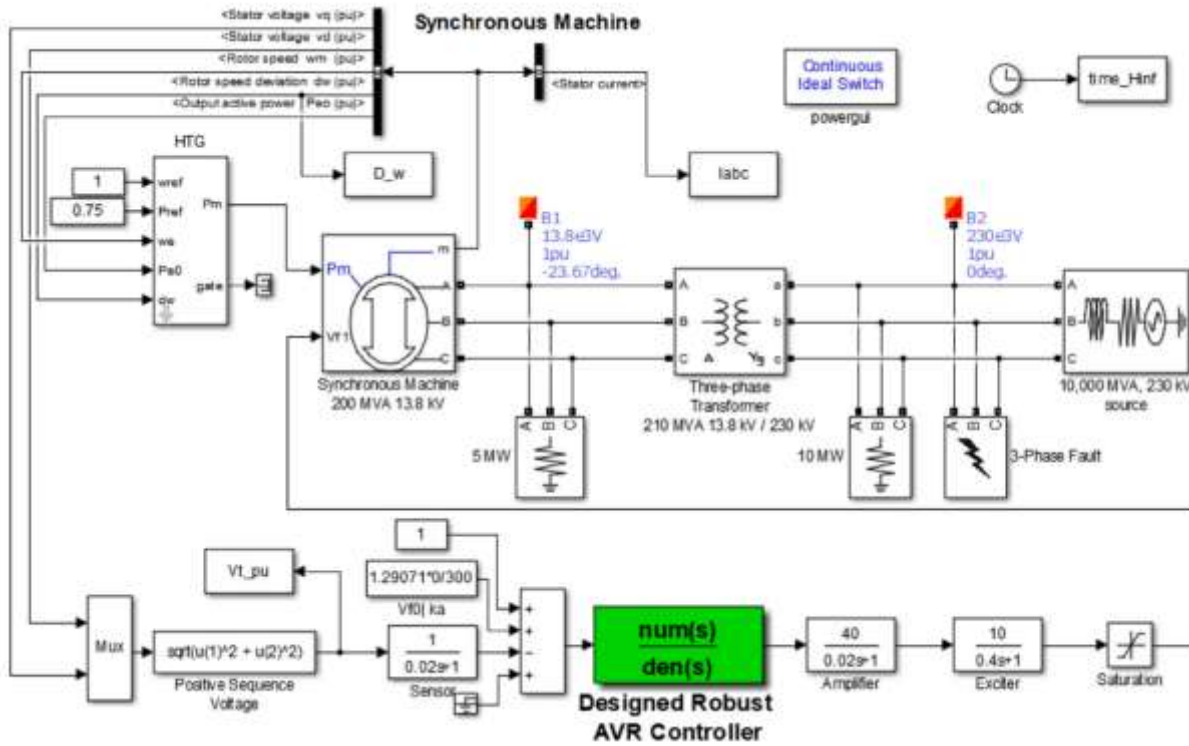


**Fig. 24:** The synchronous machine associated with the hydraulic turbine and governor (HTG) and excitation system (AVR)

### Section 3: $H^\infty$ control design (RICC & LMI)

After introducing the P- $\Delta$ -K representation of the AVR system, its nominal plant (AVR \_nom) can be constructed easily. After that, the suboptimal  $H^\infty$  controller is sketched by the nominal plant of the AVR \_ic (AVR \_nom). This nominal plant (AVR \_nom) has four inputs ([ref dist noise c]) and three outputs. The SISO suboptimal controller minimizes the infinity norm of the  $F_L$  (AVR \_nom , K) overall SISO stabilizing controllers (K) as Eq. (9). AVR \_cl =  $F_L$  (AVR \_nom , K) is the LFT of the nominal system and the designed suboptimal  $H^\infty$  controller.

$$\gamma_0 = \min_{K(s)} \|T_{zw}\|_\infty = \min_{K(s)} \|F_L(\text{AVR\_nom}, K(s))\|_\infty < \gamma < 1 \quad (9)$$

$$\text{where } z = \begin{bmatrix} y \\ y_c \end{bmatrix}, w = \begin{bmatrix} \text{ref} \\ \text{dist} \\ \text{noise} \end{bmatrix}$$

Fig. 25 shows the AVR nominal plant and its LFT representation with the controller (K) which has been designed by  $H^\infty$  optimization in MATLAB using Glover and Doyle method for a system P. Furthermore, this method determines the final gamma value achieved in controller design procedure and constructs the system closed-loop system representation (LFT of the AVR \_nom and obtained  $H^\infty$  controller or AVR \_cl).

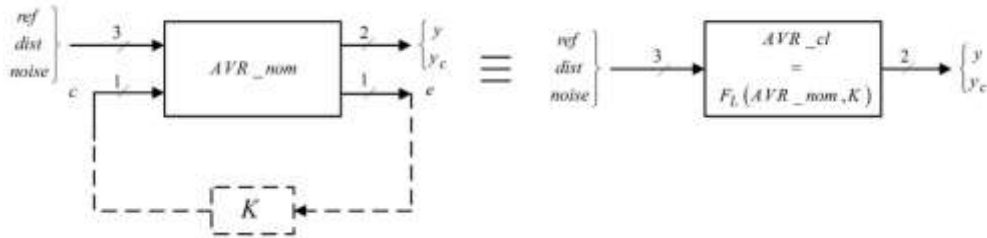


**Fig. 25:** AVR nominal plant and its LFT representation with the designed  $H^\infty$  controller

$W_p$  is the performance weighting function for the output voltage of the generator and bounds the system's sensitivity function (  $S(s) \leq W_p^{-1}(s)$  ) to create the possible small sensitivity output disturbances as:

$$W_p(s) = \frac{s+0.2}{1400s+1.2}$$

On the other hand, for confining the control system energy, the control weighting functions ( $W_u$ ) have been selected to decrease the magnitude of the controller outputs. The following structure has been chosen for  $W_u$ .

$$W_u(s) = \frac{0.1s+3}{0.1s+2.3}$$

Fig. 26 and Fig. 27 shows the magnitude curve of the reverse of the performance function ( $W_p^{-1}$ ) and control weighting function ( $W_u$ ).

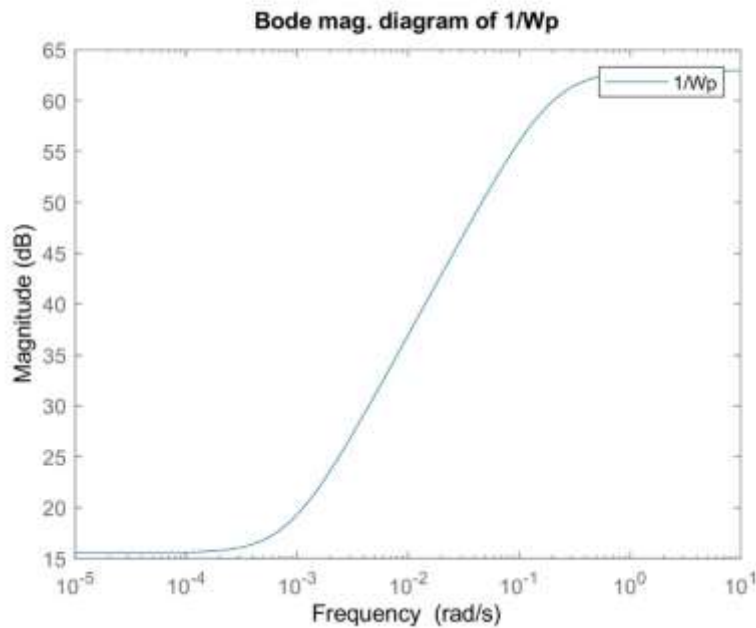


**Fig. 26:** Bode magnitude diagram of inverse of performance weighting function

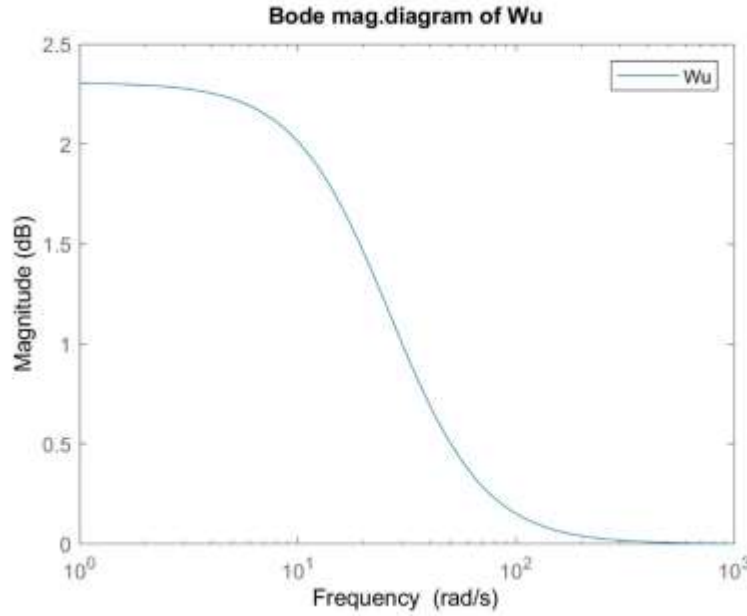


**Fig. 27:** Bode magnitude diagram of control input weighting function

The proposed strategy could be applied to power system easily by flowchart of Fig. 28. On the basis of the above procedure and the data of Table 1, a fifteen order SISO controller has been obtained and then its closed pole to the origin is converted to an origin pole like as Eq. (10) while  $\mu$  maintain its value less than one. The bode diagram of this appropriate controller is represented in Fig. 29.

$$K(s) = \frac{0.001451s^{14} + 0.2781s^{13} + 22.74s^{12} + 1032s^{11} + 2.825e4s^{10} + 4.75e5s^9 + 4.753e6s^8 + 2.593e7s^7 + 6.564e7s^6 + 8.006e7s^5 + 4.569e7s^4 + 9.824e6s^3 + 2.506e4s^2 + 21.42s + 0.006113}{s^{15} + 212.3s^{14} + 1.913e4s^{13} + 9.507e5s^{12} + 2.825e7s^{11} + 5.154e8s^{10} + 5.53e9s^9 + 3.199e10s^8 + 8.453e10s^7 + 1.081e11s^6 + 6.555e10s^5 + 1.513e10s^4 + 3.861e7s^3 + 3.301e4s^2 + 9.421s} \quad (10)$$

The nominal plant is considered as:

$$P_0 = \frac{116.8}{(0.06s+1)(0.7s+1)(1.5s+1)}$$

Where  $K_A, K_E, K_G, K_S, T_A, T_E, T_G$  and  $T_S$  are 25, 5.5, 0.85, 1, 0.06, 0.7, 1.5 and 0.0305, respectively.

The nominal plant is stable having three poles in -16.67, -1.43 and -0.67.



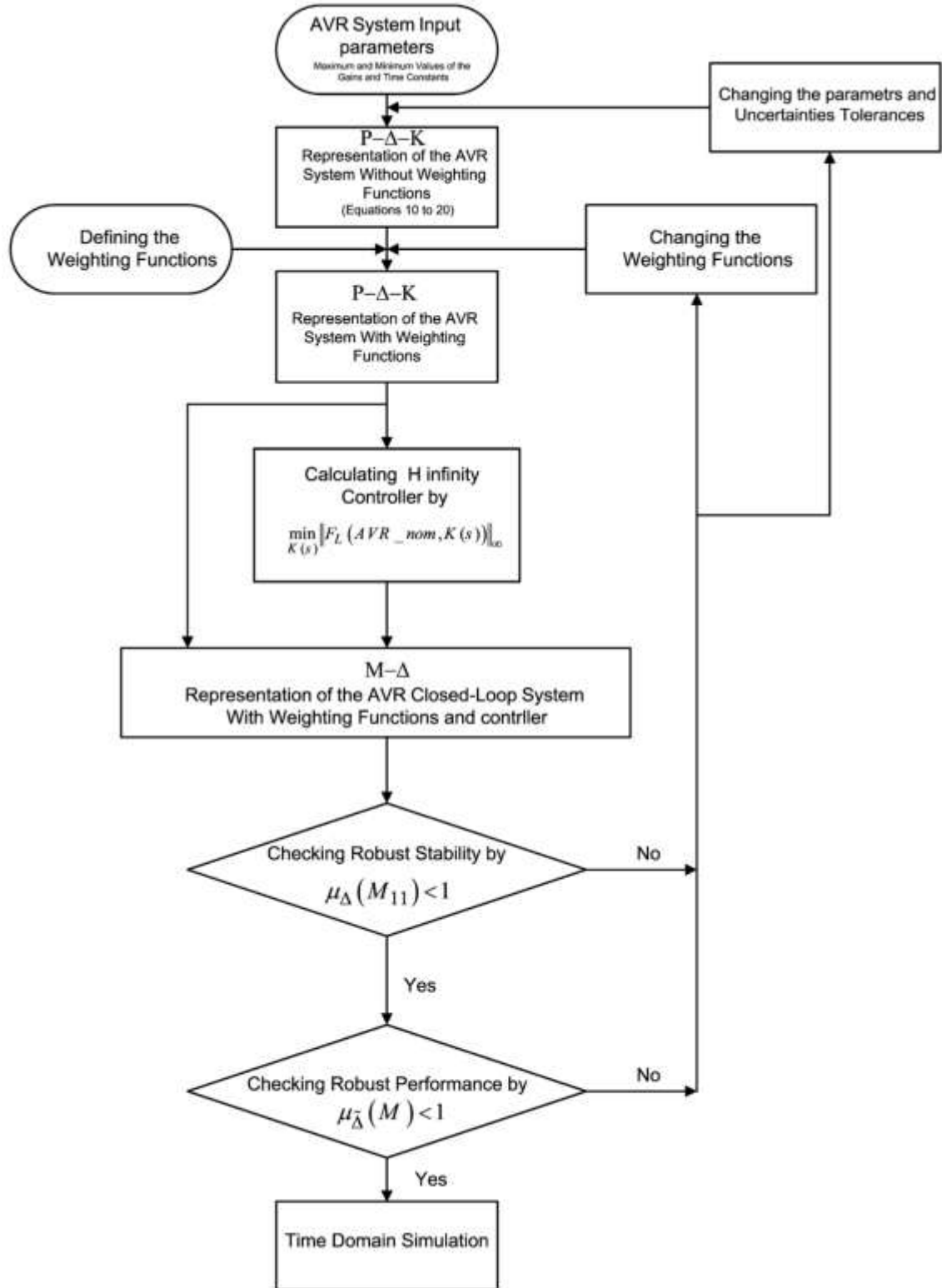


**Fig. 28:** The flowchart of the robust  $H_{\infty}$  controller design procedure for the AVR system in a large size power system

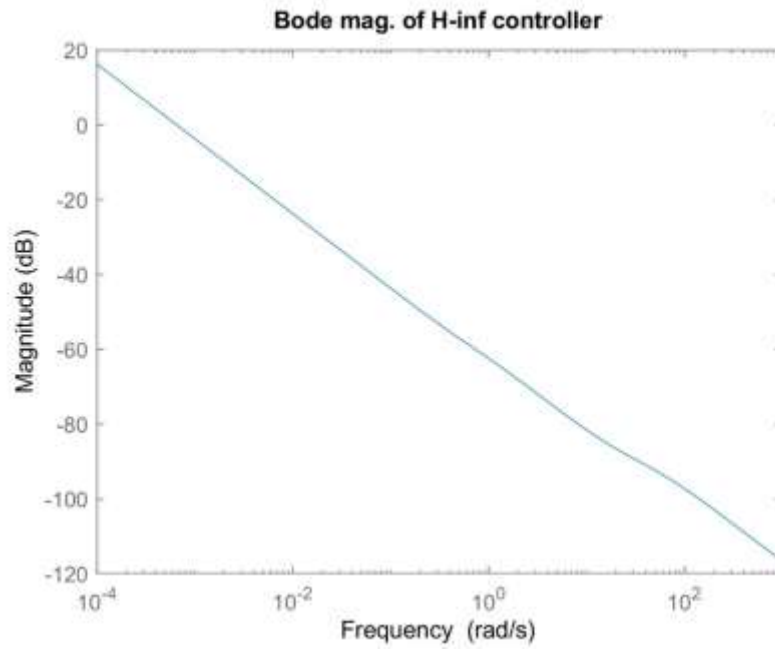


**Fig. 29:** Bode magnitude of  $H_\infty$  controller

For the case presented, the amount of  $\gamma$  is 0.0158 and the diagram of singular values of closed loop system is shown in Fig. 30. The diagram of structured singular value ( $\mu$ ) is shown in Fig. 31.

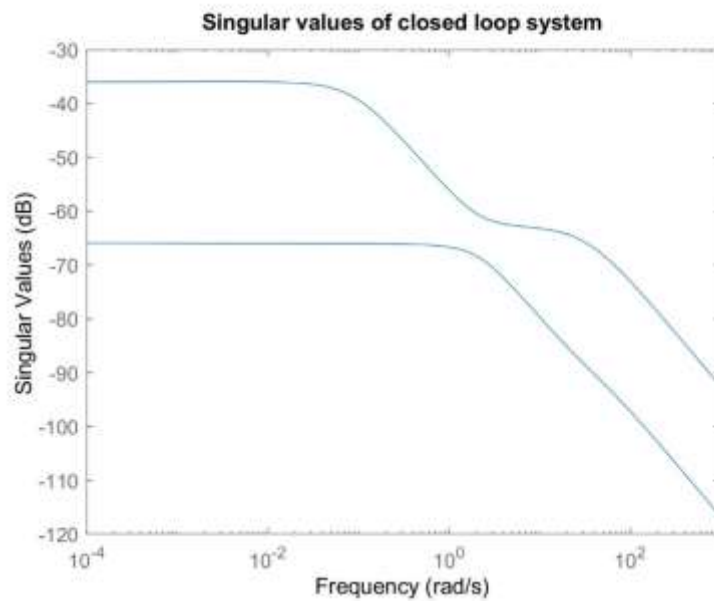


**Fig. 30:** Singular values of closed loop system

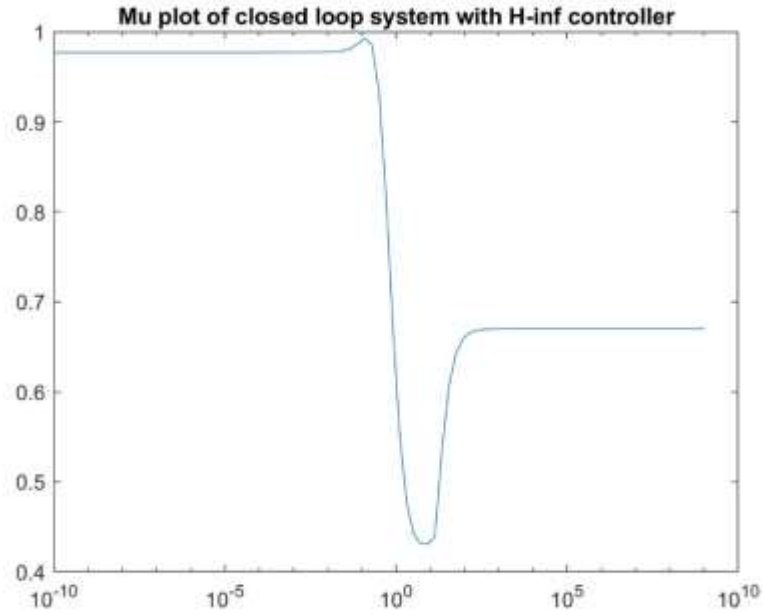


**Fig. 31:** Mu plot of closed loop system with designed  $H_\infty$  controller

In all simulations, this pattern has been considered to assess the controllers' performance:

1. There is a  $1^{pu}$  change in the reference voltage at  $t = 0$  for analyzing the tracking performance.
2. In order to analyze short circuit faults, the generator's terminal voltage will be zero by a  $-1^{pu}$  sudden disturbance at the output terminal voltage. In this case, the controllers must return the output voltage to the reference value.
3. By a sudden increment in the terminal voltage to  $2^{pu}$ , the transient overvoltage can be modeled. For this modeling a  $1^{pu}$  voltage disturbance has been added to the terminal voltage.

These patterns are applied to the AVR system in three points of functional area according to the following five scenarios:

- 1– The nominal values of time constants and gains of the transfer functions.
- 2– The maximum values of time constants and gains of the transfer functions.
- 3– The minimum values of time constants and gains of the transfer functions.

**Scenario 1:**  $KF=116.8$  ,  $TA=0.06$  ,  $TE=0.7$  ,  $TG=1.5$

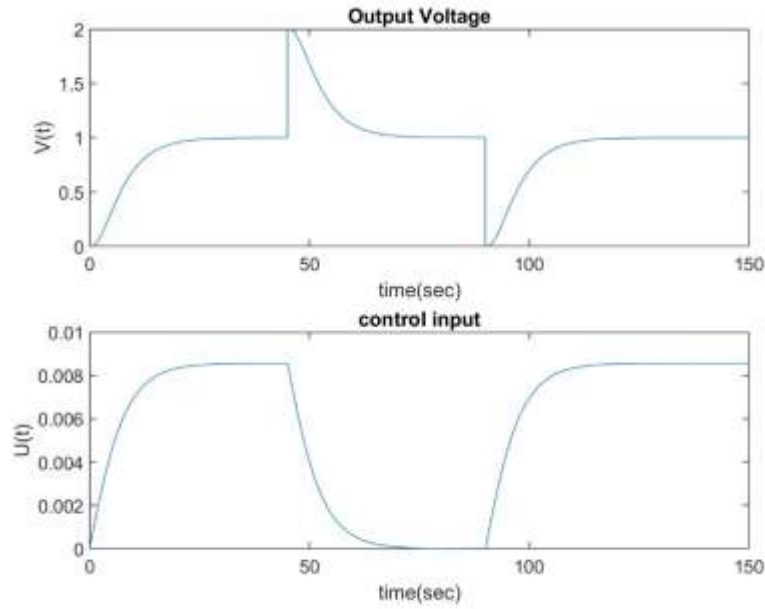


**Fig. 32:** Output voltage and control input plot for scenario 1

Fig. 32 depicts step response of closed loop system. Fig. 33 depicts step response of open loop system and Fig. 34 depicts bode magnitude diagrams of open loop and closed loop systems.

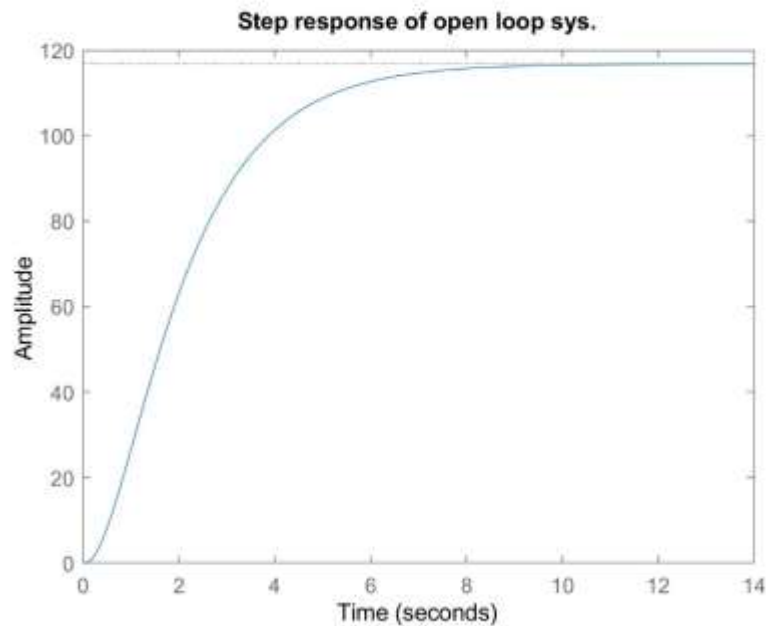


**Fig. 33:** Step response of open loop system

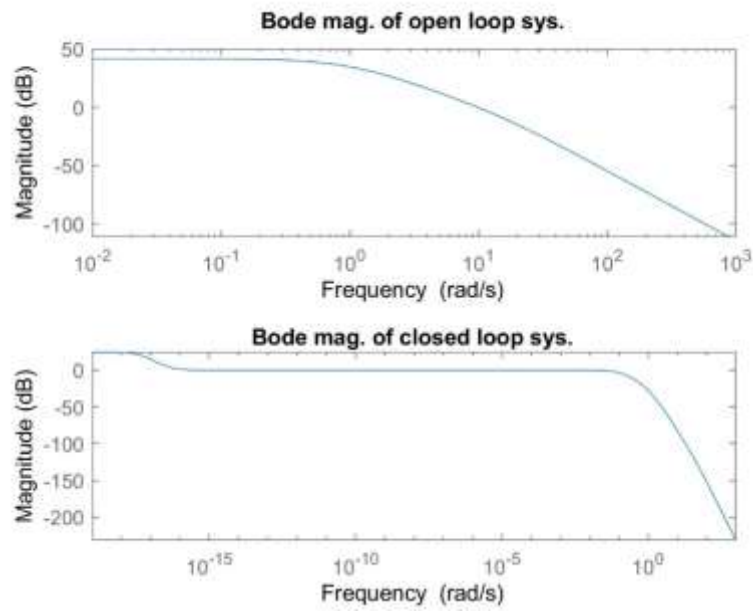


Fig. 34: Bode magnitude diagram of open loop and closed loop systems

**Scenario 2:**  $K_F=400$  ,  $T_A=0.1$  ,  $T_E=1$  ,  $T_G=2$

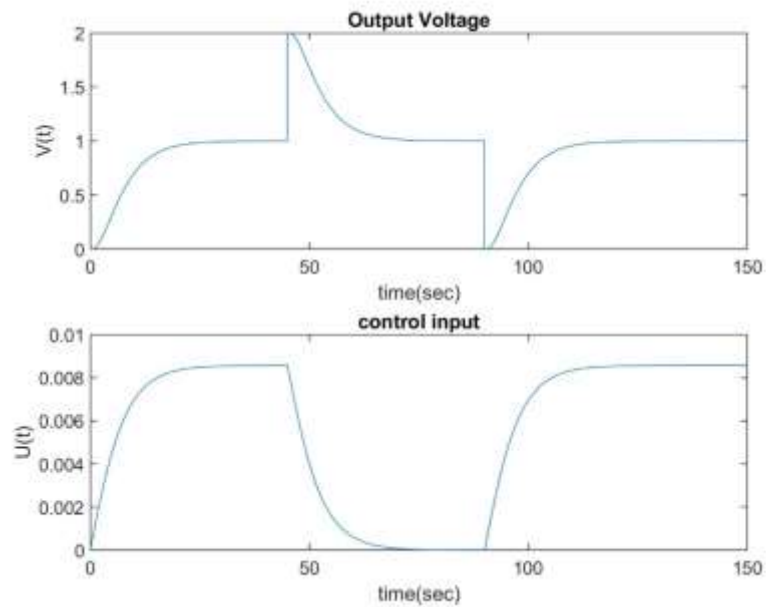
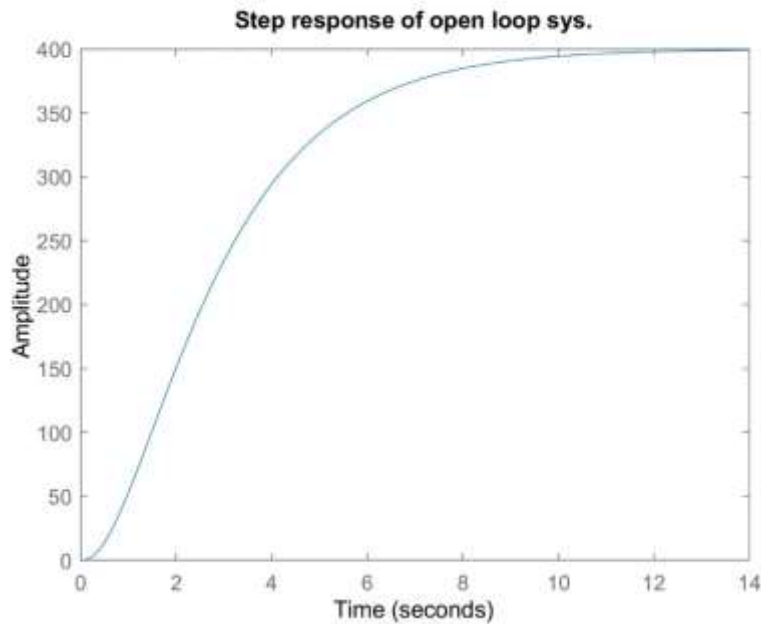
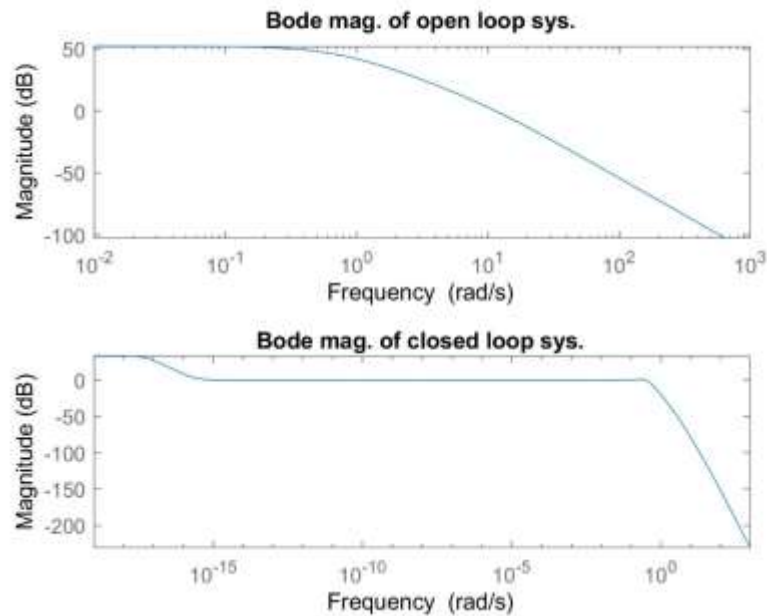


Fig. 35: Output voltage and input control plot for scenario 2

Fig. 35 depicts step response of closed loop system. Fig. 36 depicts step response of open loop system and Fig. 37 depicts bode magnitude diagrams of open loop and closed loop systems.



**Fig. 36:** Step response of open loop system



**Fig. 37:** Bode magnitude of open and closed loop systems

**Scenario 3:**  $KF=7$  ,  $TA=0.02$  ,  $TE=0.4$  ,  $TG=1$

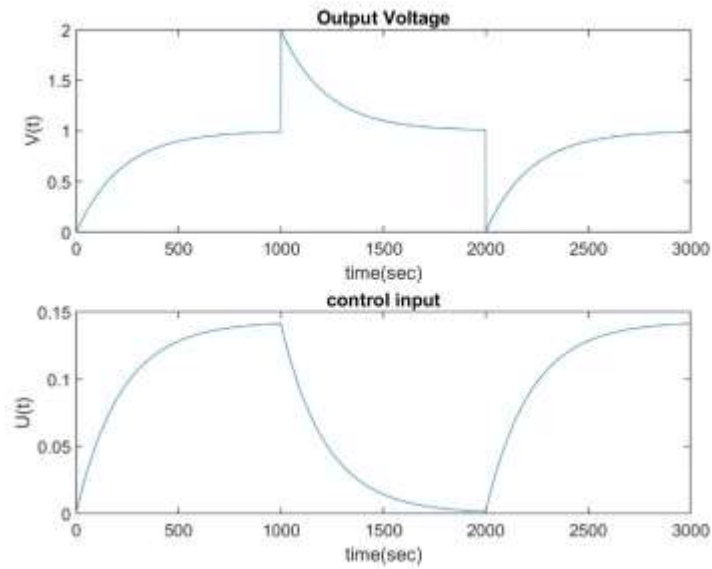


**Fig. 38:** Output voltage and input control plot for scenario 3

Fig. 38 depicts step response of closed loop system. Fig. 39 depicts step response of open loop system and Fig. 40 depicts bode magnitude diagrams of open loop and closed loop systems.

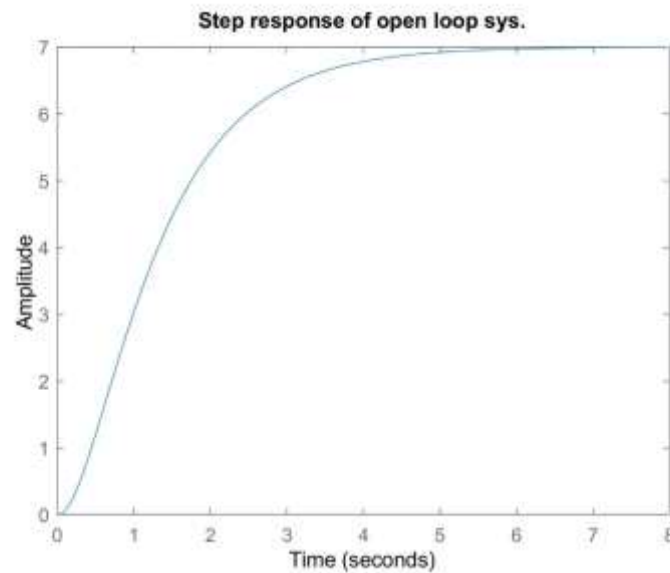


**Fig. 39:** Step response of open loop system

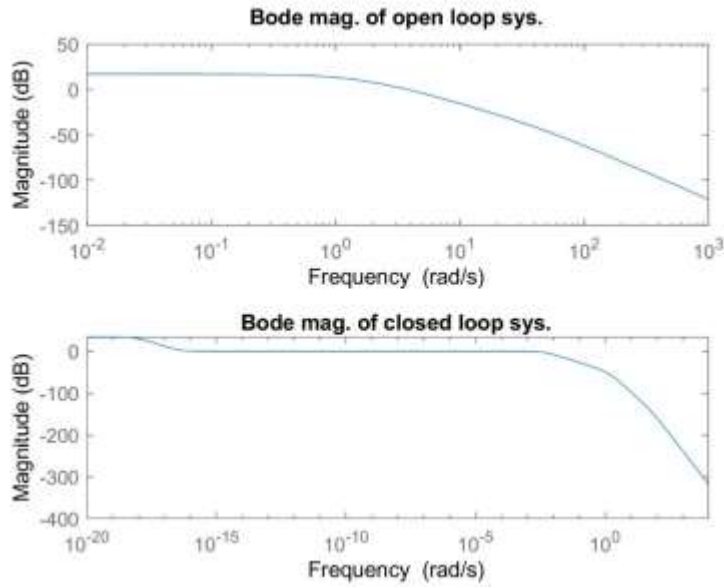


Fig. 40: Bode magnitude diagram of open and closed loop systems

The same procedure has been done to design a fifteen order  $H_\infty$  controller utilizing **LMI** method where its closed pole to the origin is converted to an origin pole like Eq. (11) while  $\mu$  maintain its value less than one. The bode diagram of this appropriate controller is represented in Fig. 41.

$K(s)=$

$$\frac{0.04376s^{14}+7.492s^{13}+534.2s^{12}+2.048e4s^{11}+4.542e5s^{10}+5.836e6s^9+4.133e7s^8+1.482e8s^7+2.82e8s^6+2.905e8s^5+1.552e8s^4+3.685e7s^3+2.257e6s^2+5.292e4s+430.3}{s^{15}+240.1s^{14}+2.423e4s^{13}+1.335e6s^{12}+4.366e7s^{11}+8.611e8s^{10}+9.913e9s^9+6.084e10s^8+1.688e11s^7+2.283e11s^6+1.508e11s^5+4.251e10s^4+2.937e9s^3+7.636e7s^2+6.81e5s} \quad (11)$$

Performance weighting function is obtained as:

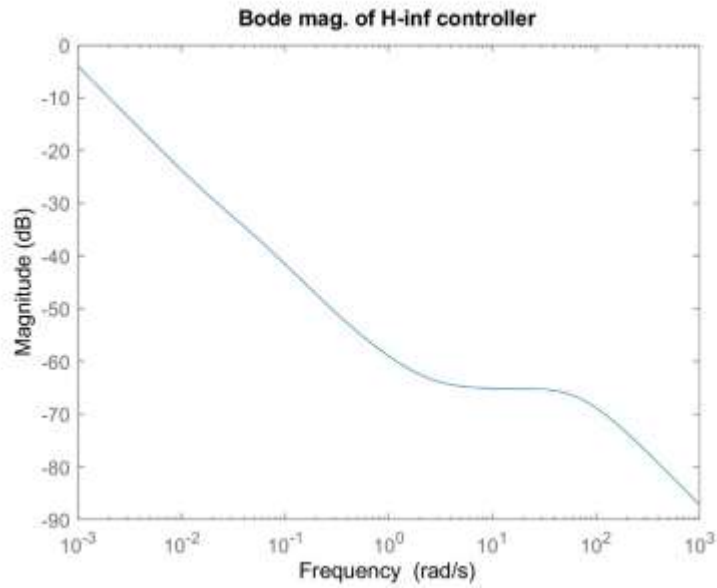
$$W_P(s)=\frac{5s+1}{1100s+28}$$

Control input weighting function is selected as:

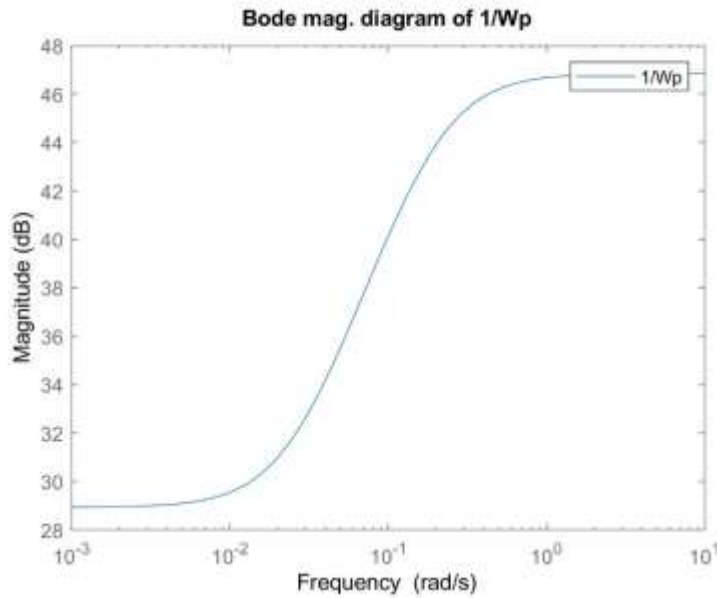
$$W_u(s)=\frac{0.1s+4.9}{s+2}$$



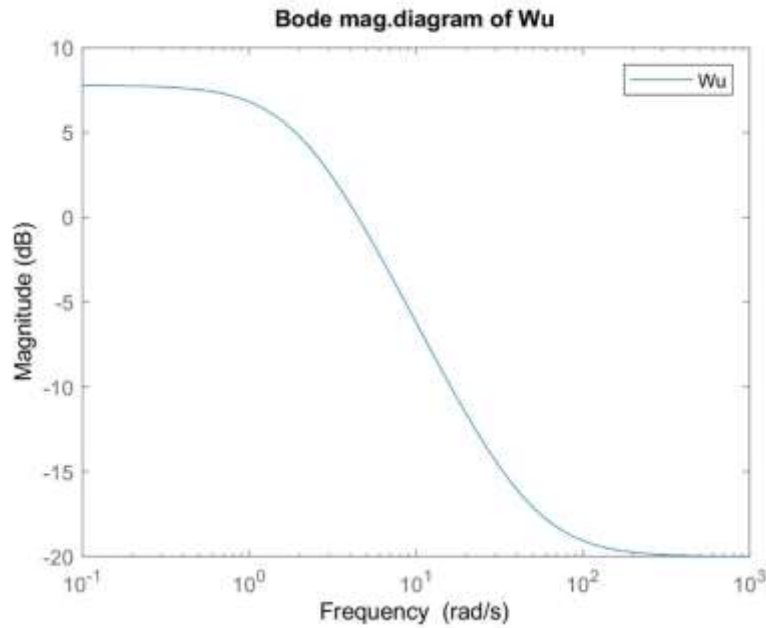
Fig. 42 and Fig. 43 shows the magnitude curve of the reverse of the performance function ( $W_p^{-1}$ ) and control weighting function ( $W_u$ ).



**Fig. 41:** Bode magnitude of designed H-inf controller with LMI method

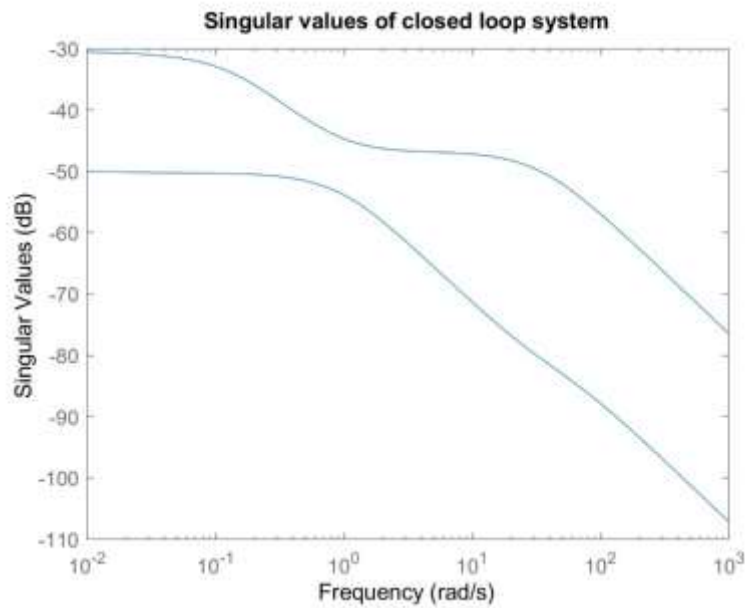


**Fig. 42:** Bode magnitude diagram of inverse of performance weighting function

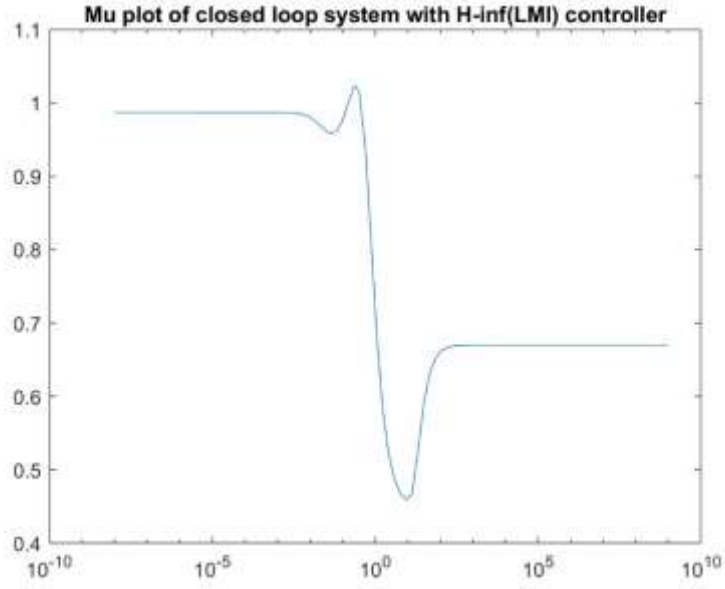


**Fig. 43:** Bode magnitude diagram of control input weighting function

For the case presented, the amount of  $\gamma$  is 0.0295 and the diagram of singular values of closed loop system is shown in Fig. 44. The diagram of structured singular value ( $\mu$ ) is shown in Fig. 45.

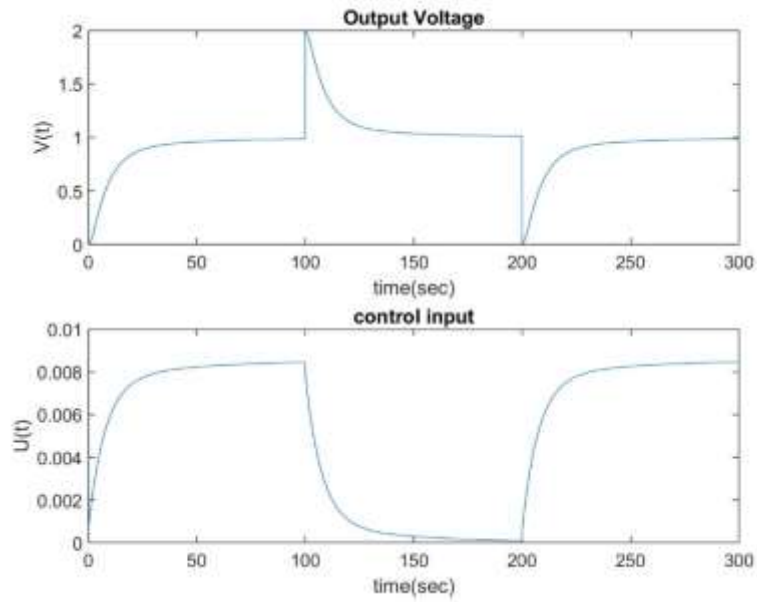


**Fig. 44:** Singular values of closed loop system



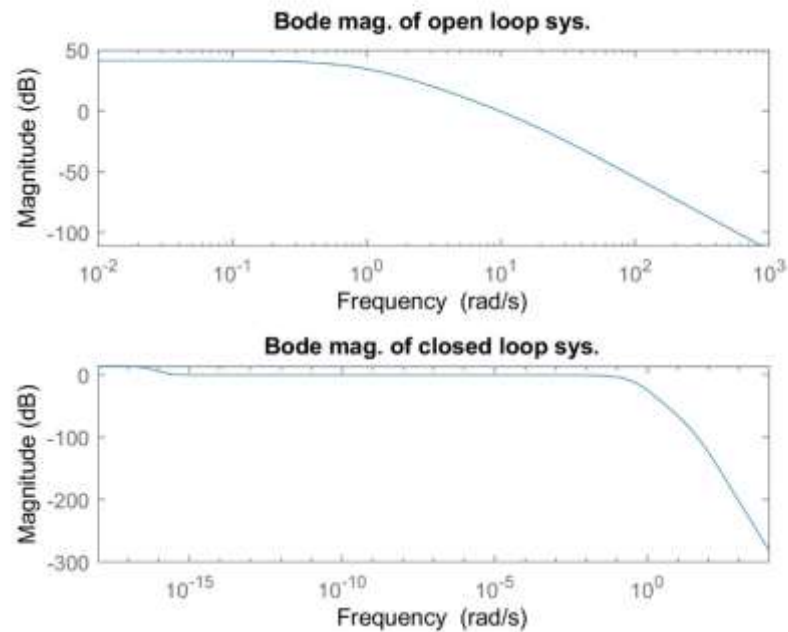
**Fig. 45:** Mu plot of closed loop system with H-inf controller utilizing LMI method

**Scenario 1:**  $KF=116.8$  ,  $TA=0.06$  ,  $TE=0.7$  ,  $TG=1.5$



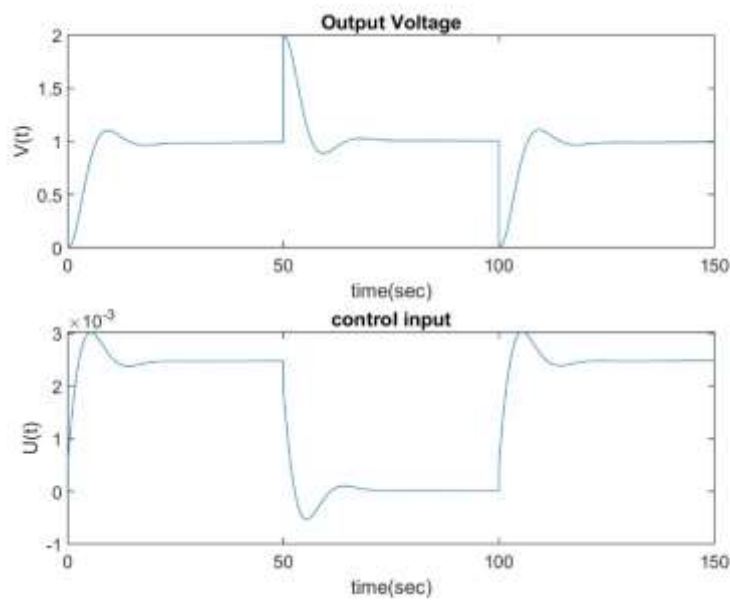
**Fig. 46:** Output voltage and control input for scenario 1

Fig. 46 depicts step response of closed loop system. Fig. 47 depicts bode magnitude diagrams of open loop and closed loop systems.



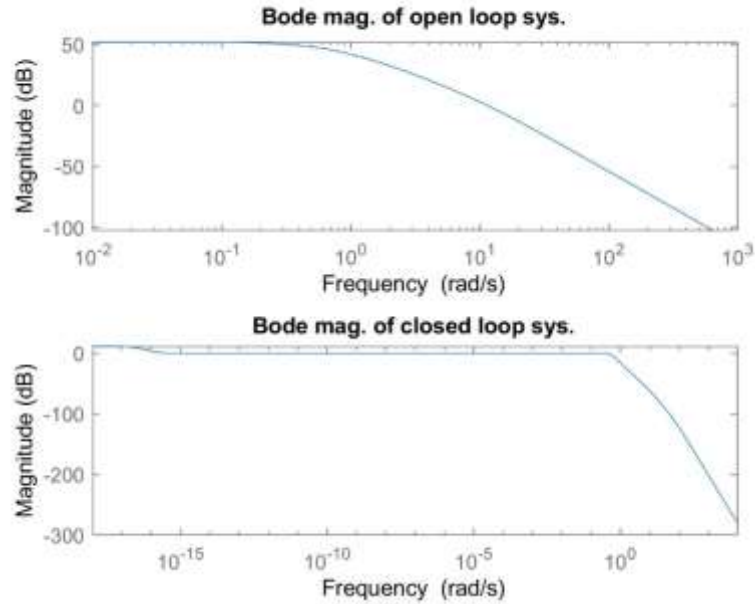
**Fig. 47:** Bode magnitude of open and closed loop systems

**Scenario 2:**  $KF=400$  ,  $TA=0.1$  ,  $TE=1$  ,  $TG=2$



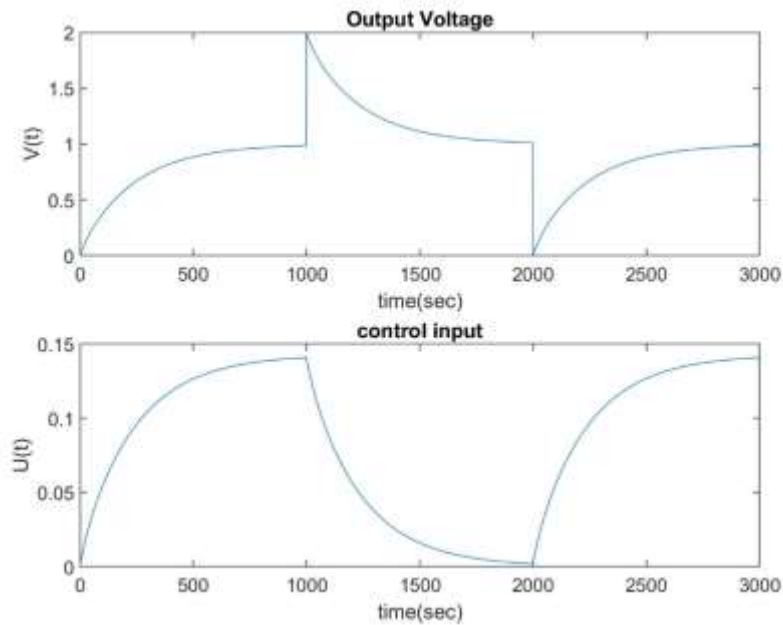
**Fig. 48:** Output voltage and control input for scenario 2

Fig. 48 depicts step response of closed loop system. Fig. 49 depicts bode magnitude diagrams of open loop and closed loop systems.



**Fig. 49:** Bode magnitude diagram of open and closed loop systems

**Scenario 3:**  $KF=7$  ,  $TA=0.02$  ,  $TE=0.4$  ,  $TG=1$



**Fig. 50:** Output voltage and control input for scenario 2

Fig. 50 depicts step response of closed loop system. Fig. 51 depicts bode magnitude diagrams of open loop and closed loop systems.

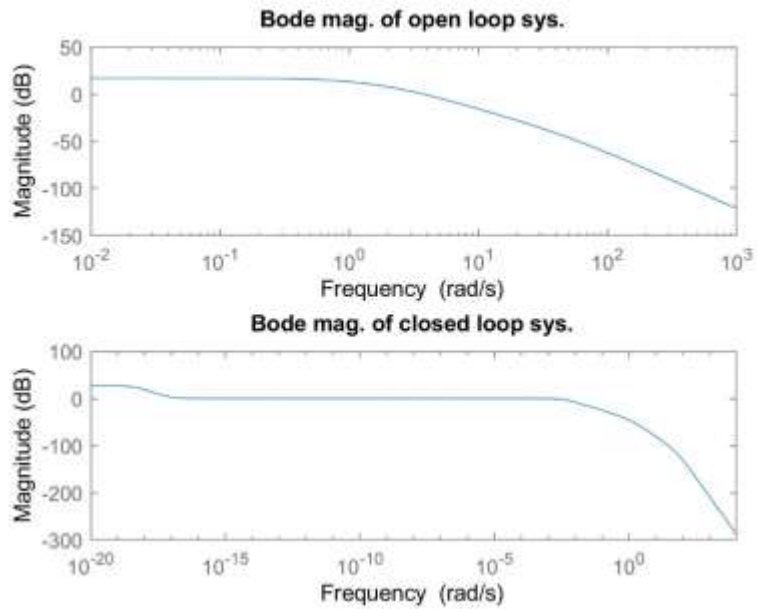


**Fig. 51:** Bode magnitude diagram of open and closed loop systems

## Simulation a real synchronous generator connected to a 230 kV network

Here, as in previous section, a 200 MVA, 13.8 kV, 112.5 rpm generator has been studied which is linked to a 230 kV network via a Delta-Y 210 MVA transformer.

Fig. 52 and 53 represent the deviation of the voltage terminal magnitude by the  $H_\infty$  controller, designed via riccati method. Fig. 54 and 55 represent the deviation of the voltage terminal magnitude by the  $H_\infty$  controller, designed via lmi method.

**Scenario 1 (RICC) :**  $KA=40$  ,  $KE=10$  (maximum)

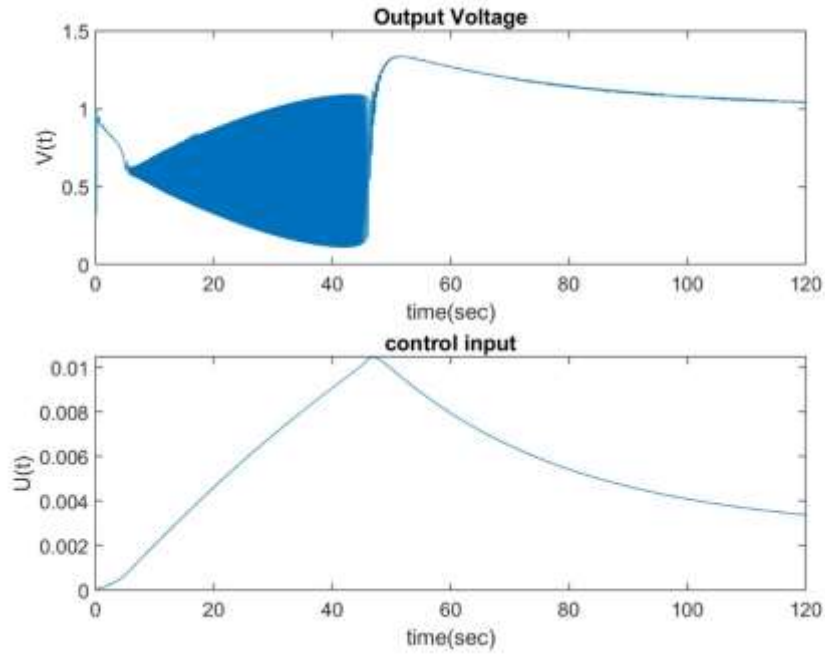


**Fig. 52:** Terminal voltage and control input for scenario 1

**Scenario 2 (RICC) :**  $KA=10$  ,  $KE=1$  (minimum)

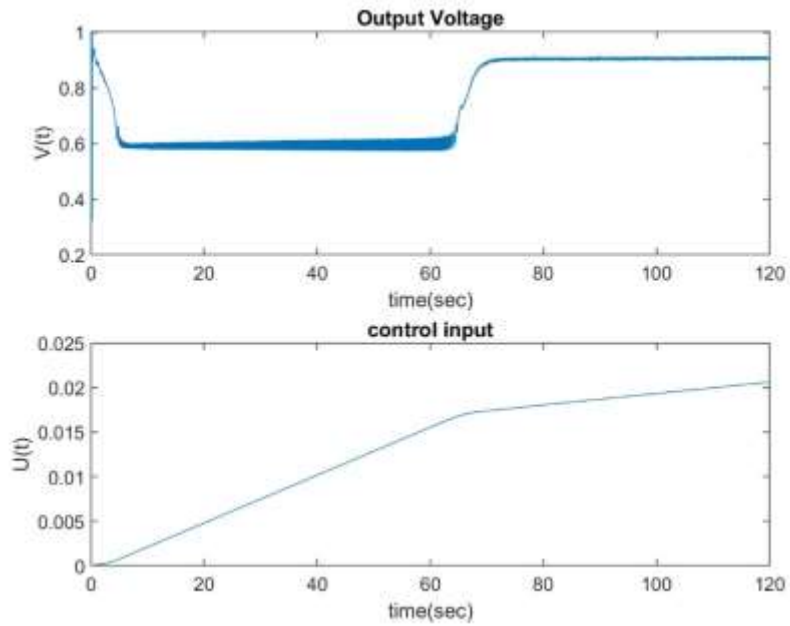


**Fig. 53:** Terminal voltage and control input for scenario 2

**Scenario 1 (LMI) :**  $K_A=40$  ,  $K_E=10$  (maximum)

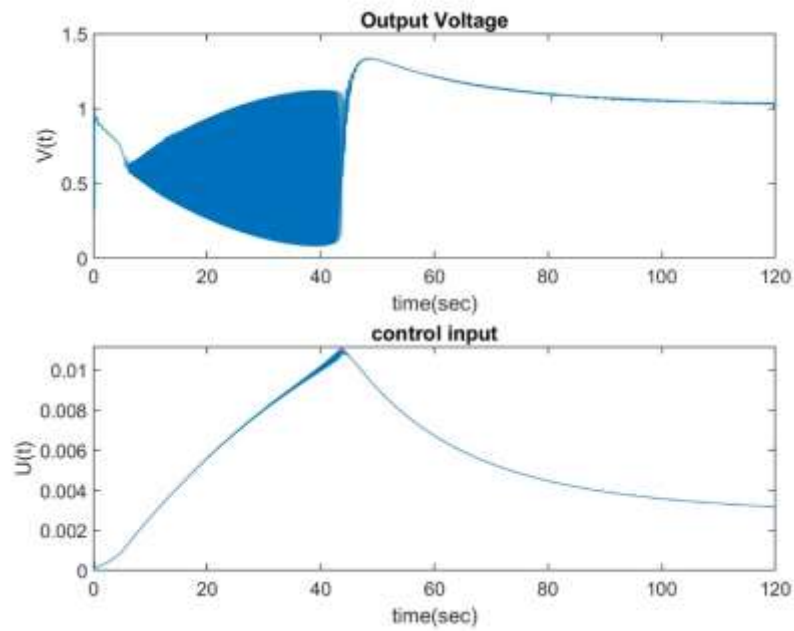


**Fig. 54:** Terminal voltage and control input for scenario 1

**Scenario 2 (RICC) :**  $K_A=10$  ,  $K_E=1$  (minimum)

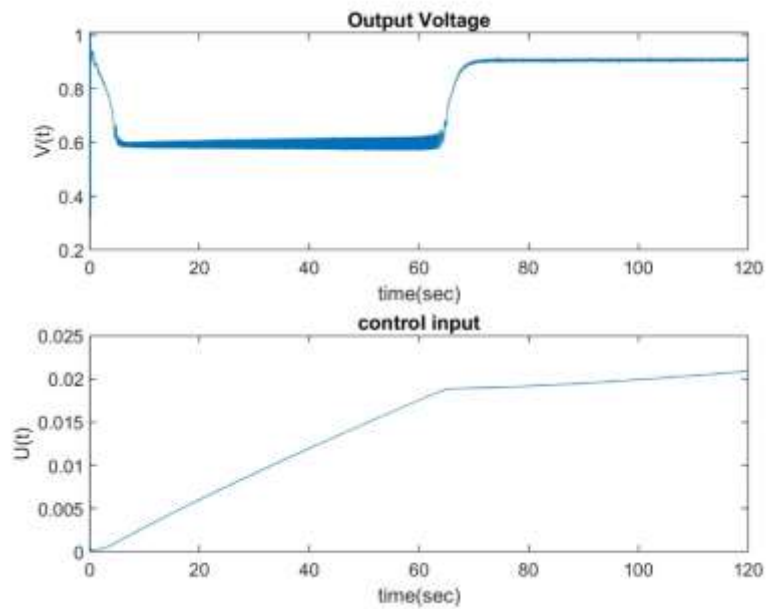


**Fig. 55:** Terminal voltage and control input for scenario 2



## Section 4: H2 control design

The same procedure as in previous section has been done to design a fourteen order H2 controller. Controller order could be reduced to eleven like as Eq.(12) by appropriate reduction method and then its closed pole to the origin is converted to an origin pole while  $\mu$  maintain its value fairly less than one. The bode diagram of this appropriate controller is represented in Fig. 56.

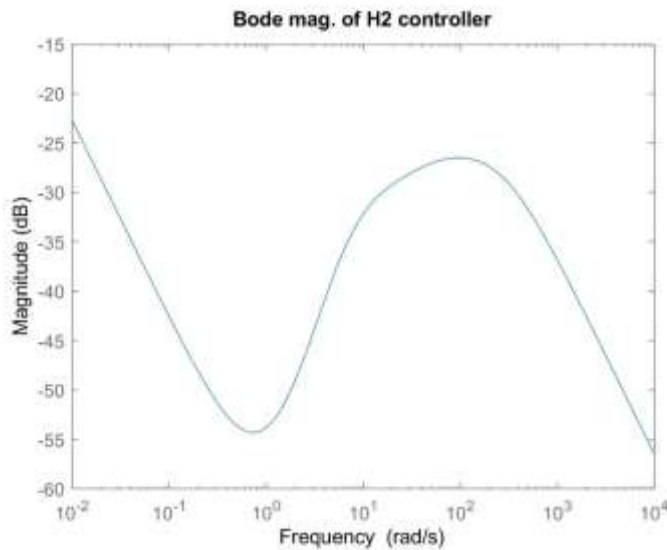
$$K(s) = \frac{14.9s^{10} + 2056s^9 + 1.15e5s^8 + 3.353e6s^7 + 5.475e7s^6 + 5.037e8s^5 + 2.511e9s^4 + 6.321e9s^3 + 8.143e9s^2 + 5.117e9s + 1.231e9}{s^{11} + 445.5s^{10} + 5.714e4s^9 + 3.504e6s^8 + 1.203e8s^7 + 2.473e9s^6 + 3.118e10s^5 + 2.392e11s^4 + 1.06e12s^3 + 3.352e12s^2 + 1.678e12s} \quad (11)$$

Performance weighting function is obtained as:

$$W_P(s) = \frac{s+18}{10s+100}$$

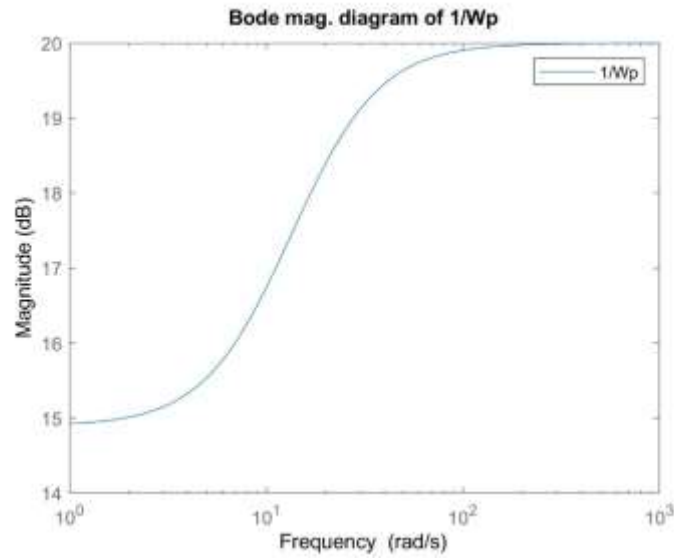
Control input weighting function is selected as:

$$W_u(s) = \frac{s+280}{80s+100}$$

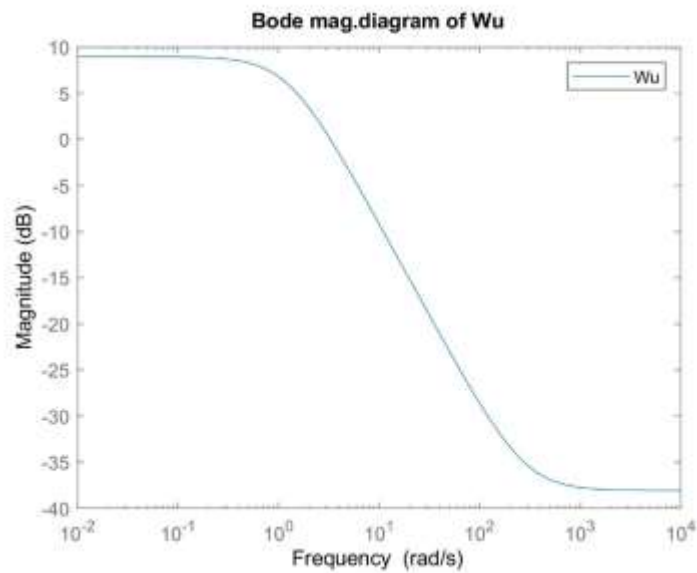


**Fig. 56:** Bode magnitude of designed H2 controller

Fig. 57 and Fig. 58 shows the magnitude curve of the reverse of the performance function ( $W_p^{-1}$ ) and control weighting function ( $W_u$ ).

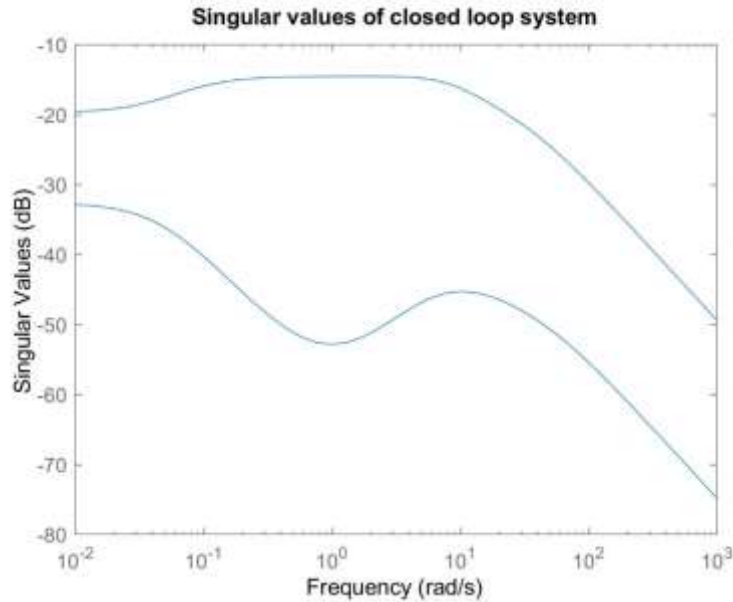


**Fig. 57:** Bode magnitude diagram of inverse of performance weighting function

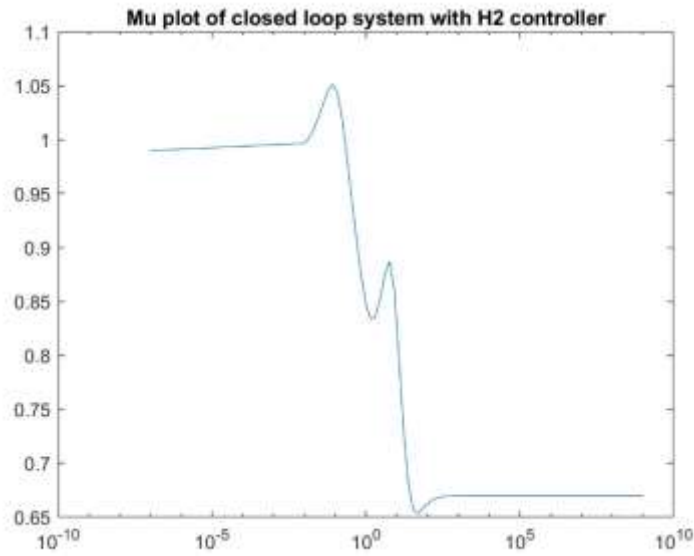


**Fig. 58:** Bode magnitude diagram of control input weighting function

For the case presented, the amount of  $\gamma$ , the norm 2 of closed loop system, is 0.5315. The diagram of singular values of closed loop system is shown in Fig. 59 and the diagram of structured singular value ( $\mu$ ) is shown in Fig. 60.

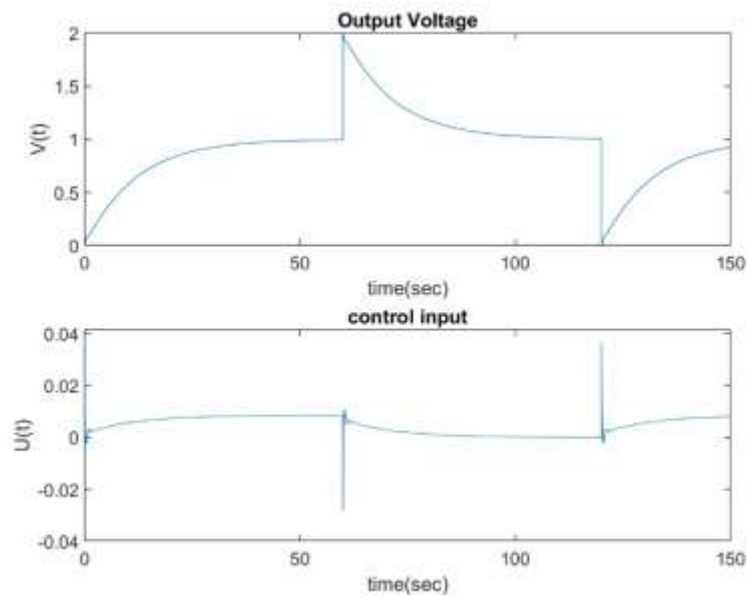


**Fig. 59:** Singular values of closed loop system



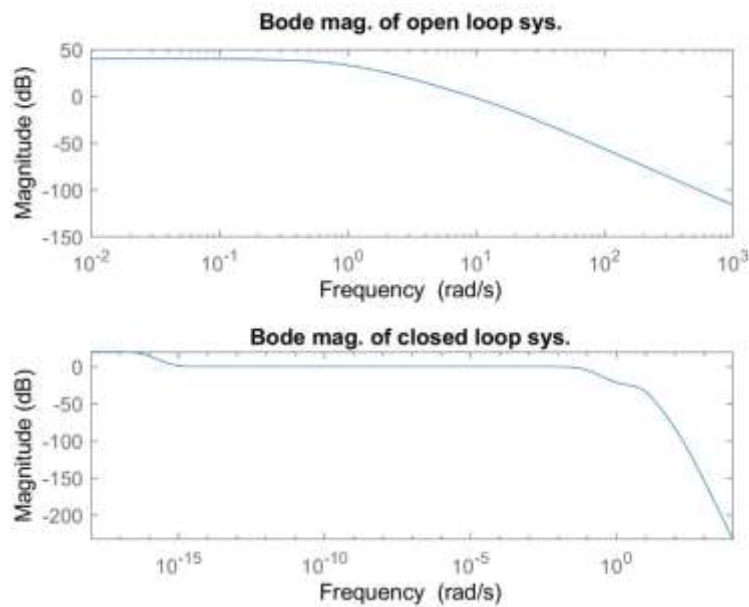
**Fig. 60:** Mu plot of closed loop system with H2 controller

**Scenario 1:**  $KF=116.8$  ,  $TA=0.06$  ,  $TE=0.7$  ,  $TG=1.5$



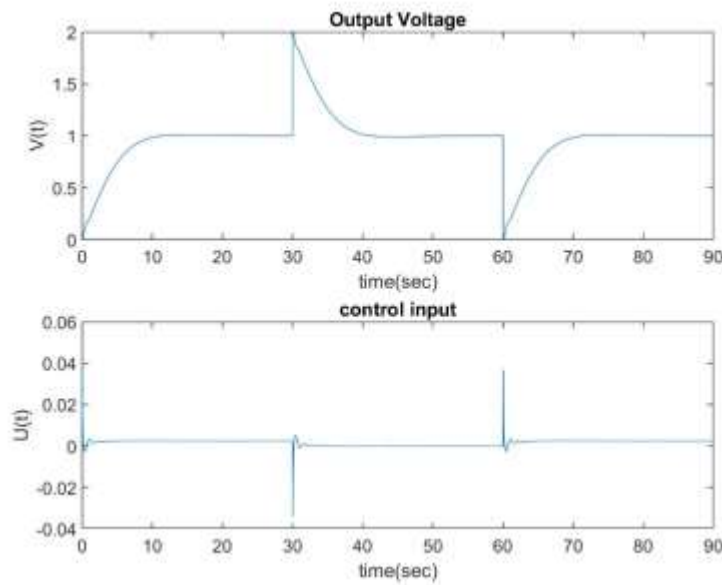
**Fig. 61:** Output voltage and control input for scenario 1

Fig. 61 depicts step response of closed loop system. Fig. 62 depicts bode magnitude diagrams of open loop and closed loop systems.



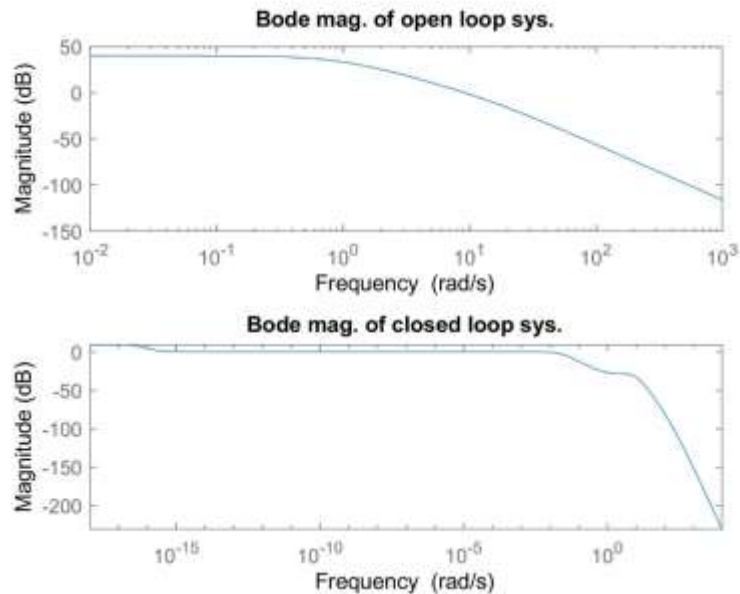
**Fig. 62:** Bode magnitude diagram of open and closed loop systems

**Scenario 2:**  $KF=400$  ,  $TA=0.1$  ,  $TE=1$  ,  $TG=2$



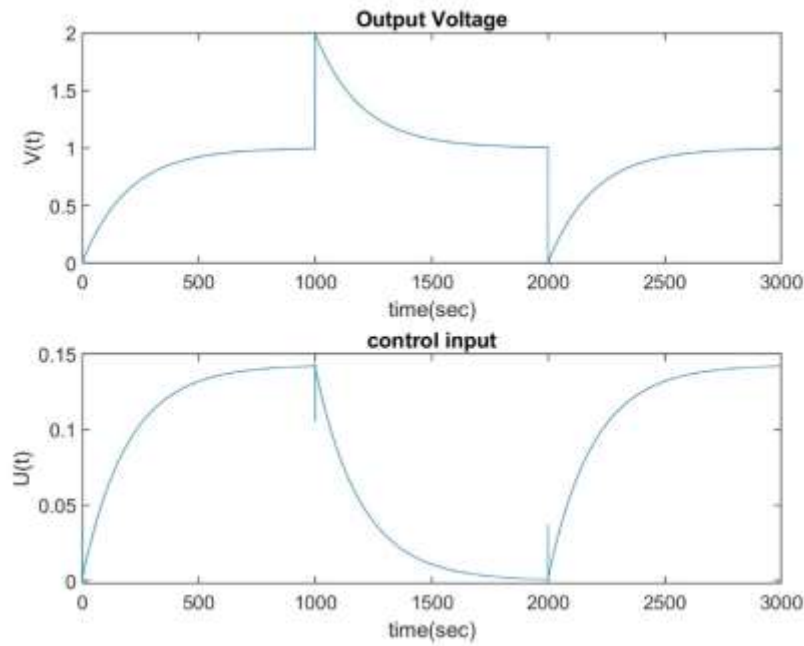
**Fig. 63:** Output voltage and control input for scenario 1

Fig. 63 depicts step response of closed loop system. Fig. 64 depicts bode magnitude diagrams of open loop and closed loop systems.



**Fig. 64:** Bode magnitude of open and closed loop systems

**Scenario 3:**  $KF=7$  ,  $TA=0.02$  ,  $TE=0.4$  ,  $TG=1$



**Fig. 65:** Output voltage and control input for scenario 3

Fig. 65 depicts step response of closed loop system. Fig. 66 depicts bode magnitude diagrams of open loop and closed loop systems.

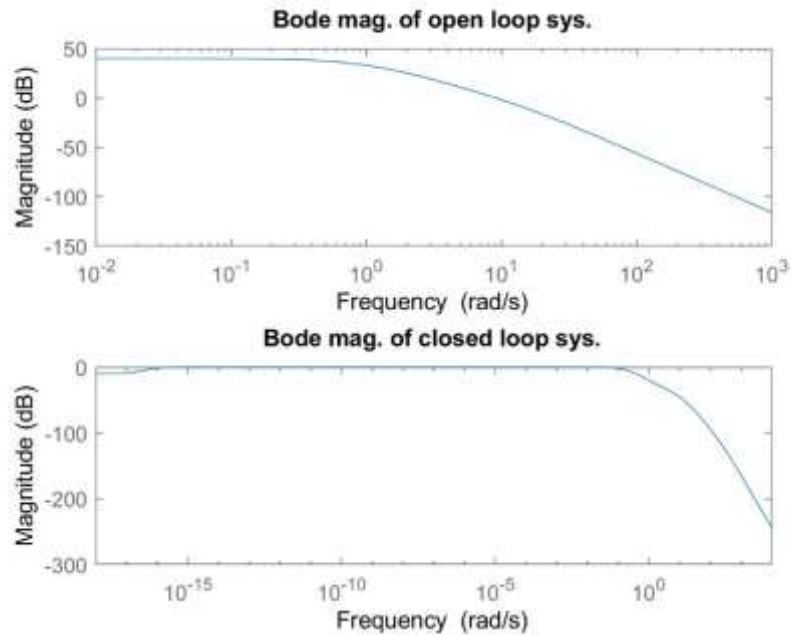


**Fig. 66:** Bode magnitude diagram of open and closed loop systems

## Simulation a real synchronous generator connected to a 230 kV network

Fig. 67 and 68 represents the deviation of the voltage terminal by the  $H_2$  controller.

**Scenario 1:**  $KA=40$  ,  $KE=10$  (maximum)

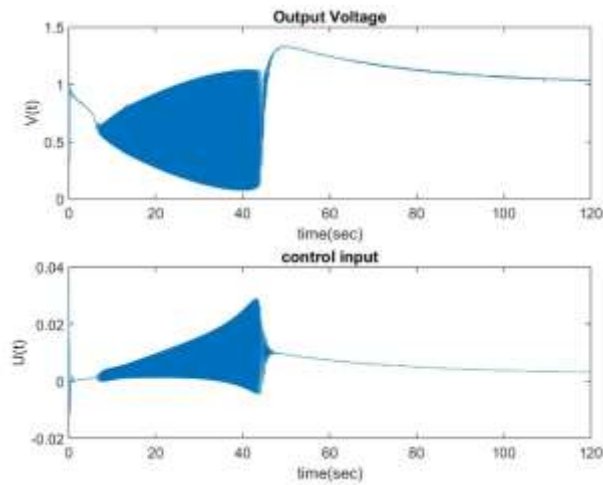


**Fig. 67:** Terminal voltage and control input for scenario 1

**Scenario 2:**  $KA=10$  ,  $KE=1$  (minimum)

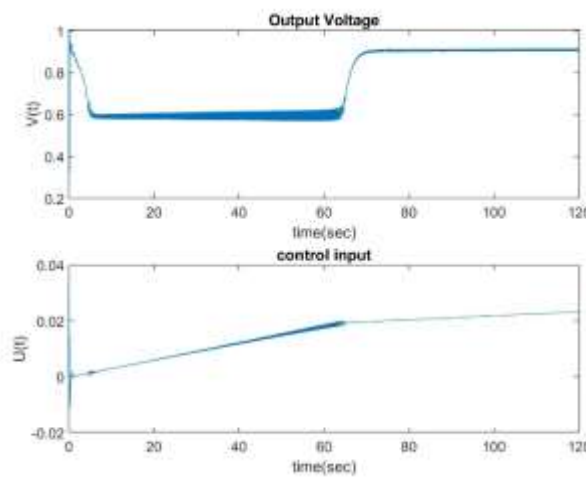


**Fig. 68:** Terminal voltage and control input for scenario 2

## Section 5: H2/H $\infty$ control design

The same procedure as in section 2 has been done to design a fourteen order H2/H $\infty$  controller like as Eq. (12) but the plant has partitioned state-space form given by:

$$\dot{x} = Ax + B_1w + B_2u$$

$$z_\infty = C_1x + D_{11}w + D_{12}u$$

$$z_2 = C_2x + D_{21}w + D_{22}u$$

$$y = C_yx + D_{y1}w + D_{y2}u$$

The resulting controller K minimizes the  $H_\infty$  norm G of the transfer function from w to  $z_\infty$  and the  $H_2$  norm H of the transfer function from w to  $z_2$ . The controller minimizes a trade-off criterion of the form  $G^2 + H^2$ .

$$K(s) = \frac{-0.0005932s^{13} - 0.08217s^{12} - 3.963s^{11} - 47.82s^{10} + 2433s^9 + 1.041e5s^8 + 1.64e6s^7 + 1.167e7s^6 + 3.294e7s^5 + 4.235e7s^4 + 2.486e7s^3 + 5.421e6s^2 + 6485s + 1.945}{s^{14} + 200s^{13} + 1.653e4s^{12} + 7.365e5s^{11} + 1.929e7s^{10} + 3.049e8s^9 + 2.886e9s^8 + 1.603e10s^7 + 5.162e10s^6 + 9.263e10s^5 + 8.123e10s^4 + 2.551e10s^3 + 1.523e7s^2 - 9168s - 5.486} \quad (12)$$

The bode diagram of this appropriate controller is represented in Fig. 69.

Performance weighting function is obtained as:

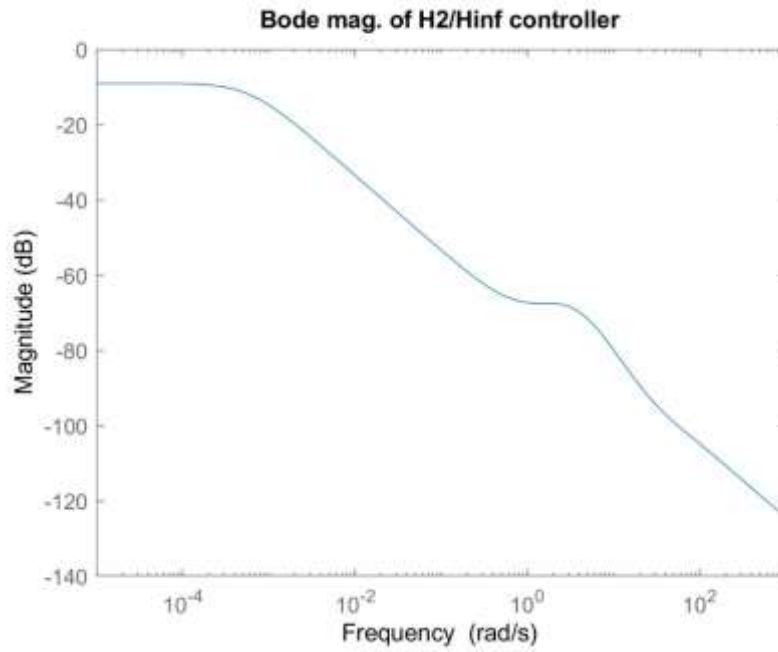
$$W_P(s) = \frac{s+0.3}{500s+0.3}$$

Control input weighting function is selected as:

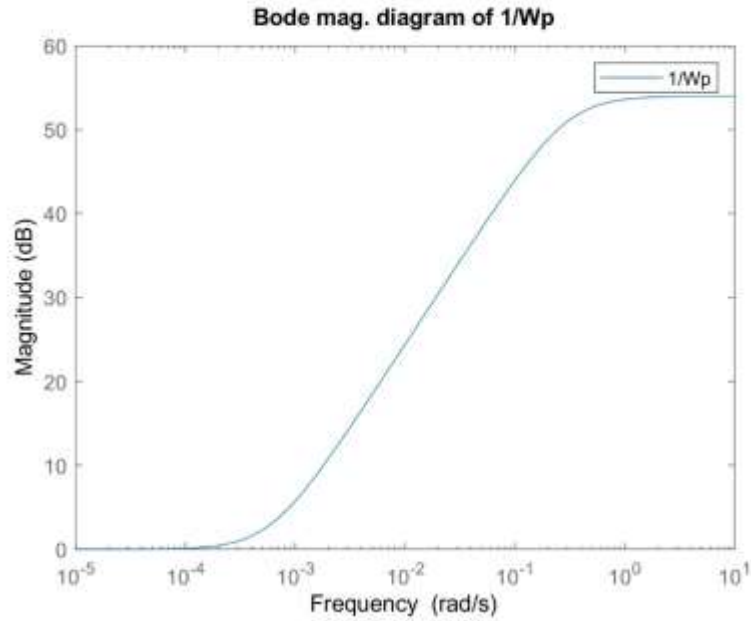
$$W_u(s) = \frac{s+4.5}{3s+2.8}$$

Fig. 70 and Fig. 71 shows the magnitude curve of the reverse of the performance function ( $W_p^{-1}$ ) and control weighting function ( $W_u$ ).



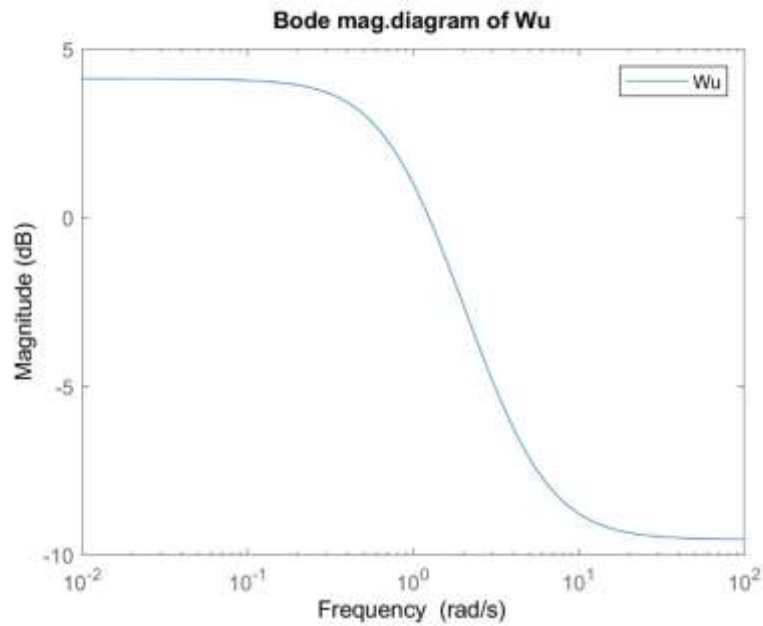


**Fig. 69:** Bode magnitude diagram of designed H2/Hinf controller

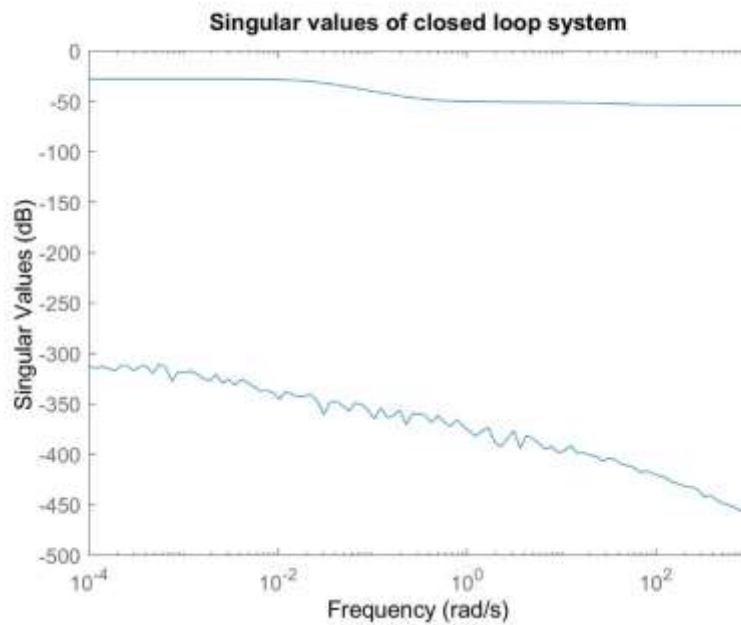


**Fig. 70:** Bode magnitude diagram of inverse of performance weighting function

For the case presented, the two amounts of  $\gamma$  are [0.0586 0.0111] and the diagram of singular values of closed loop system is shown in Fig. 72.

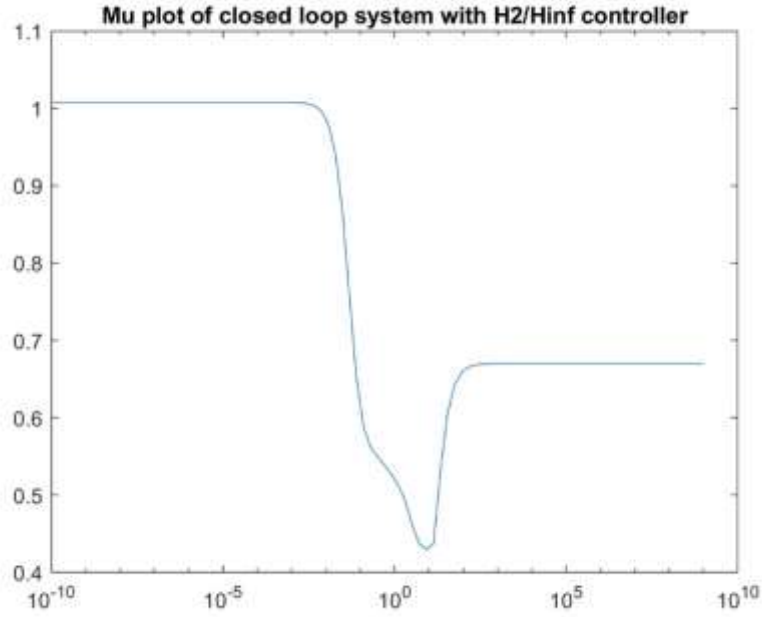


**Fig. 71:** Bode magnitude diagram of control input weighting function



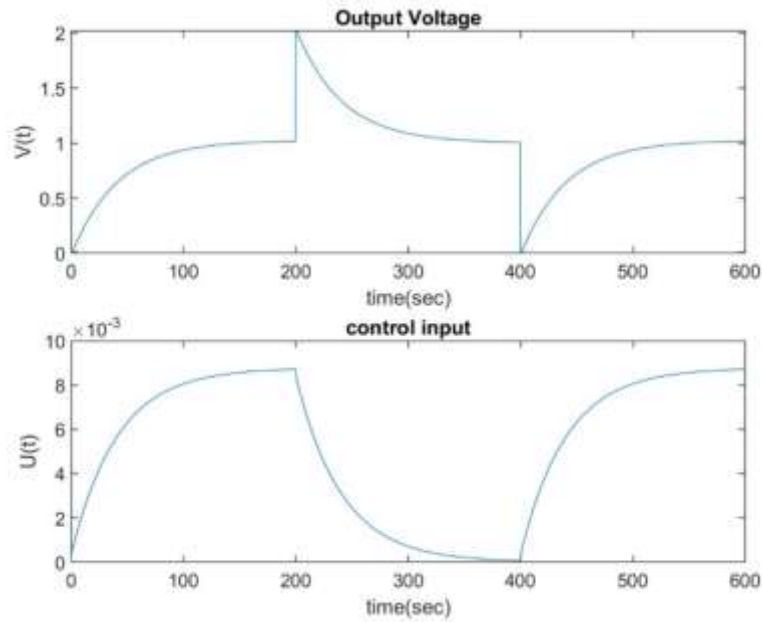
**Fig. 72:** Singular values of closed loop system

The diagram of structured singular value ( $\mu$ ) is shown in Fig. 73 where the value of  $\mu$  is fairly less than one which could guarantee robust performance of closed loop system.



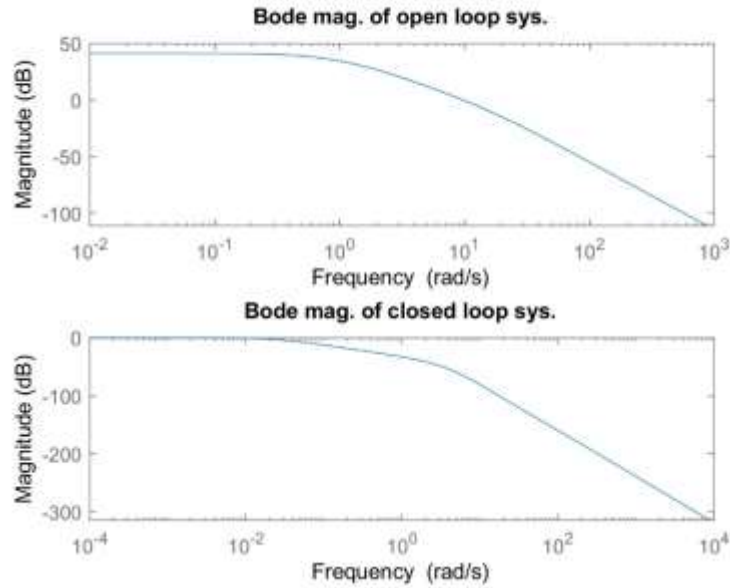
**Fig. 73:** Mu plot of closed loop system with designed H2/Hinf controller

**Scenario 1:**  $KF=116.8$  ,  $TA=0.06$  ,  $TE=0.7$  ,  $TG=1.5$



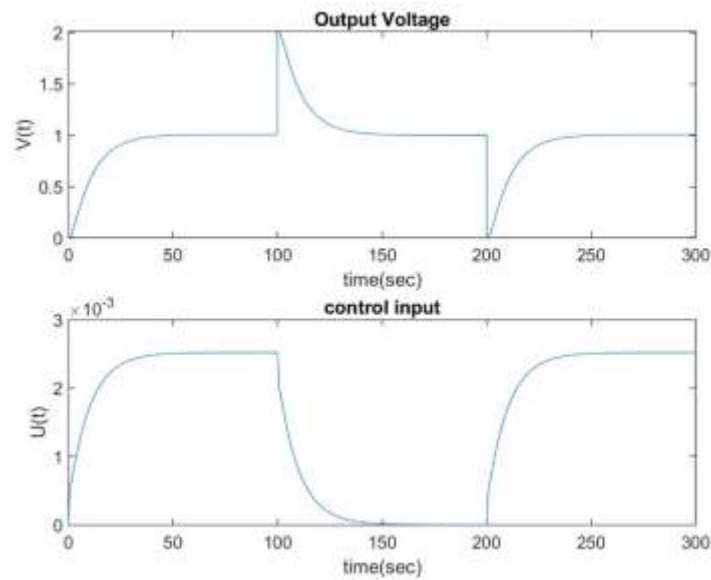
**Fig. 74:** Output voltage and control input for scenario 1

Fig. 74 depicts step response of closed loop system. Fig. 75 depicts bode magnitude diagrams of open loop and closed loop systems.



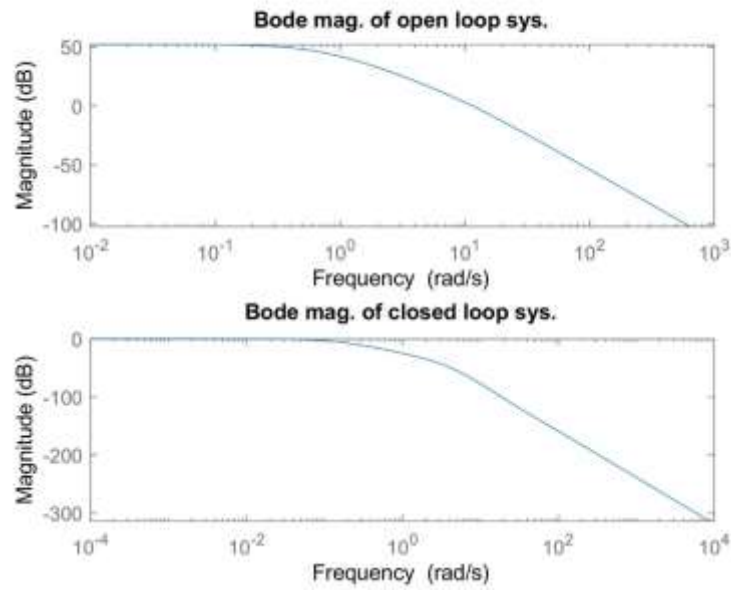
**Fig. 75:** Bode magnitude diagram of open and closed loop systems

**Scenario 2:**  $KF=400$  ,  $TA=0.1$  ,  $TE=1$  ,  $TG=2$



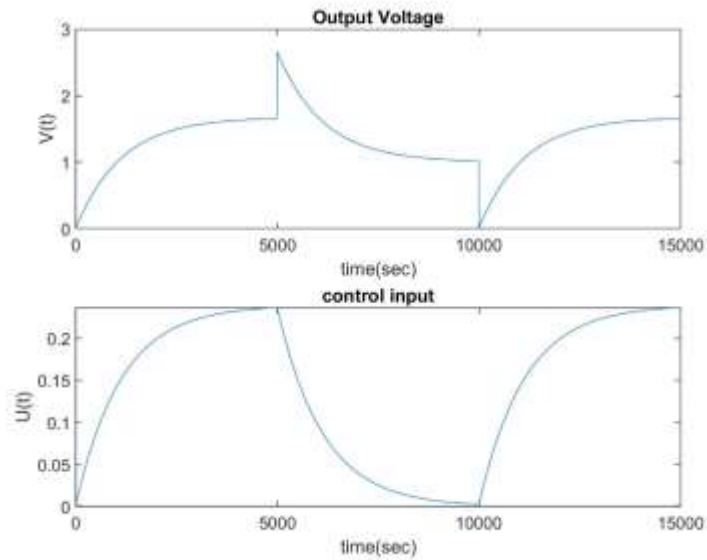
**Fig. 76:** Output voltage and control input for scenario 2

Fig. 76 depicts step response of closed loop system. Fig. 77 depicts bode magnitude diagrams of open loop and closed loop systems.



**Fig. 77:** Bode magnitude diagram of open and closed loop systems

**Scenario 3:**  $KF=7$  ,  $TA=0.02$  ,  $TE=0.4$  ,  $TG=1$



**Fig. 78:** Output voltage and control input for scenario 3

Fig. 78 depicts step response of closed loop system. Fig. 79 depicts bode magnitude diagrams of open loop and closed loop systems.

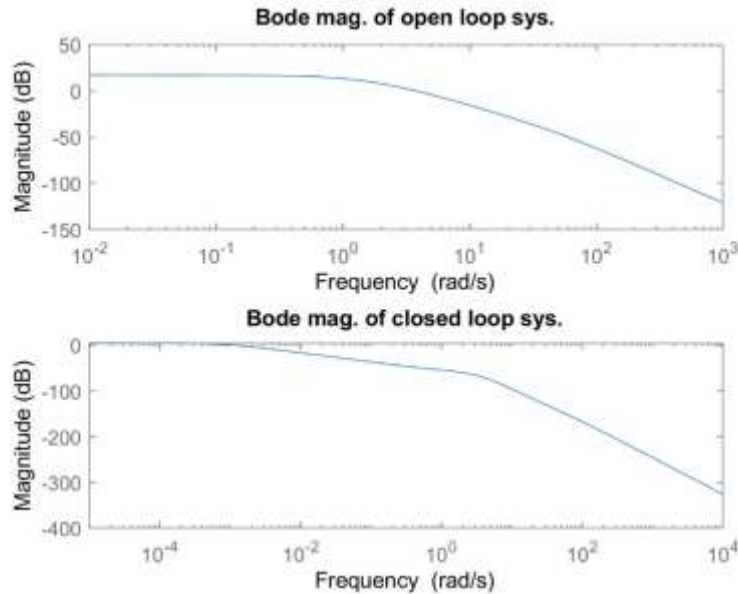


**Fig. 79:** Bode magnitude diagram of open and closed loop systems

## Simulation a real synchronous generator connected to a 230 kV network

Here, as in previous section, a 200 MVA, 13.8 kV, 112.5 rpm generator has been studied which is linked to a 230 kV network via a Delta-Y 210 MVA transformer. Fig. 80 and 81 represent the deviation of the voltage terminal magnitude by the  $H_\infty$  controller, designed via riccati method. Fig. 54 and 55 represent the deviation of the voltage terminal magnitude by the  $H_2/H_\infty$  controller, designed via lmi method.

**Scenario 1:**  $K_A=40$  ,  $K_E=10$  (maximum)

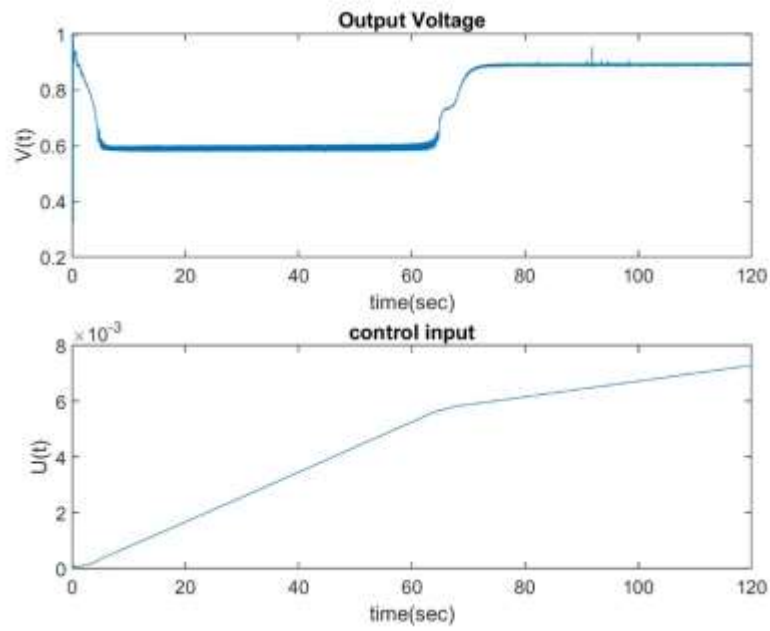


**Fig. 80:** Terminal voltage and control input for scenario 1

**Scenario 2:**  $K_A=10$  ,  $K_E=1$  (minimum)

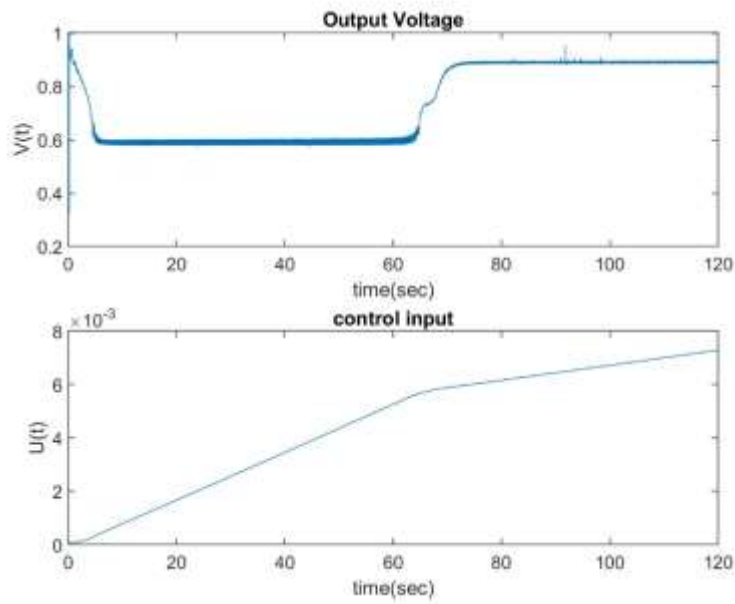


**Fig. 81:** Terminal voltage and control input for scenario 2

## Section 6: Parametric controller design

In this section,  $P$  is already stable and we parameterize all  $C$ s for which the feedback system is internally stable (Fig. 82). Most synthesis problems can be formulated in this way: Given  $P$ , design  $C$  so that the feedback system (1) is internally stable, and (2) acquires some additional desired property; for example, the output  $y$  asymptotically tracks a step input  $r$ . The method of solution is to parameterize all  $C$ s for which (1) is true, and then to see if there exists a parameter for which (2) holds.

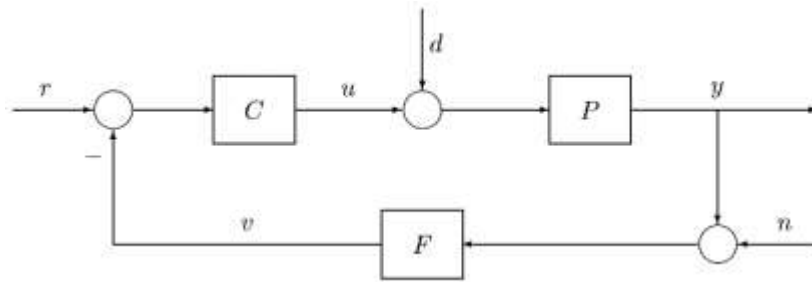


Fig. 82: Basic feedback loop

The set of all  $C$ s for which the feedback system is internally stable equals:

$$\left\{ \frac{Q}{1-PQ} : Q \in S \right\}$$

The symbol  $S$  is introduced for the family of all stable, proper, real-rational functions.

Output  $y$  asymptotically tracks a step iff the transfer function from  $r$  to  $e$  has a zero at  $s=0$ , that is,

$$P(0)Q(0)=1 \tag{12}$$

The relation (12) could also maintain the rejection of step output disturbance.

Here,  $Q$  is assumed as  $\frac{s+1}{s+a}$ , so  $a$  could be calculated as below:

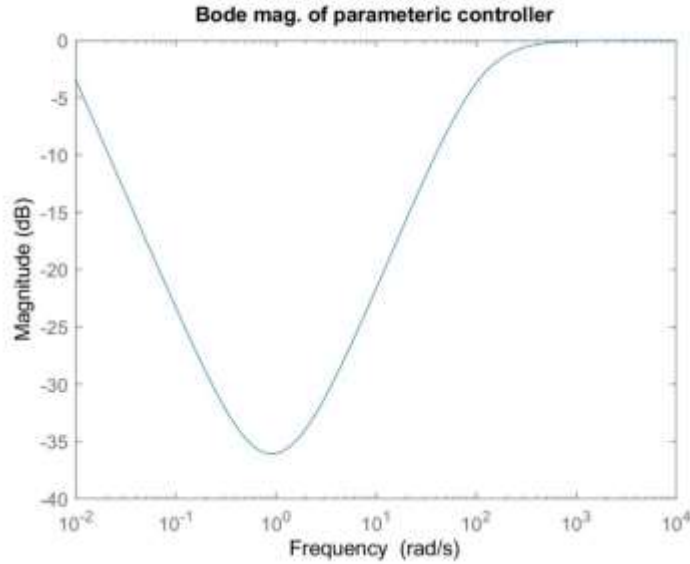
$$P(s) = \frac{116.8}{(0.06s+1)(0.7s+1)(1.5s+1)} \rightarrow P(0)=116.8$$



$$Q(0) = \frac{1}{a} = \frac{1}{116.8} \rightarrow a = 116.8 \rightarrow Q(s) = \frac{s+1}{s+116.8}$$

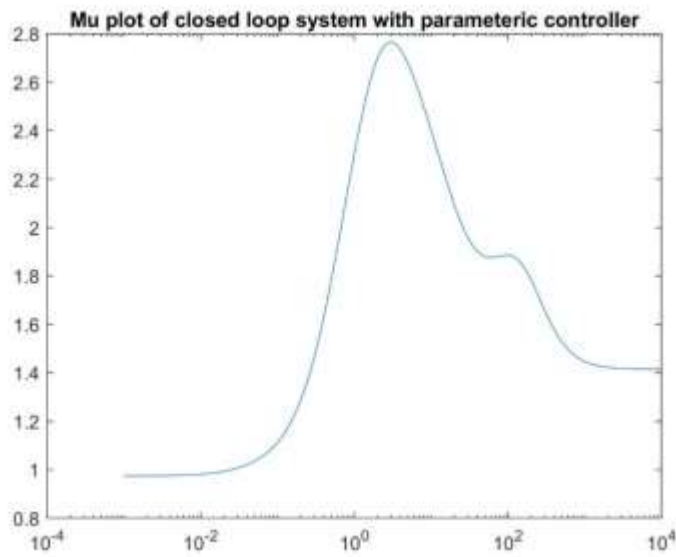
The parametric controller is obtained as Eq. (13). The bode diagram of controller has been shown in Fig. 83.

$$C(s) = \frac{0.063s^4 + 1.245s^3 + 3.442s^2 + 3.26s + 1}{0.063s^4 + 8.54s^3 + 140.3s^2 + 148.2s} \quad (13)$$



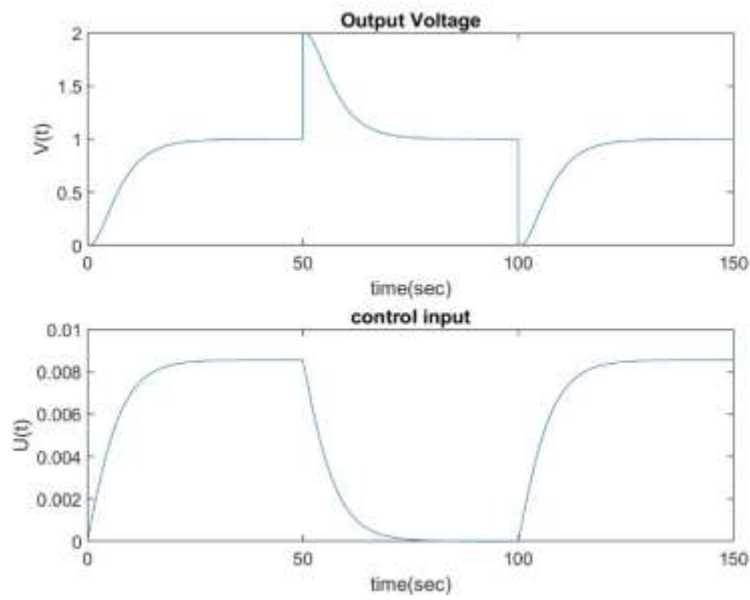
**Fig. 83:** Bode magnitude diagram of parametric controller

The diagram of structured singular value is shown in Fig. 84. The amount of  $\mu$  is above one, so robust performance is not guaranteed.



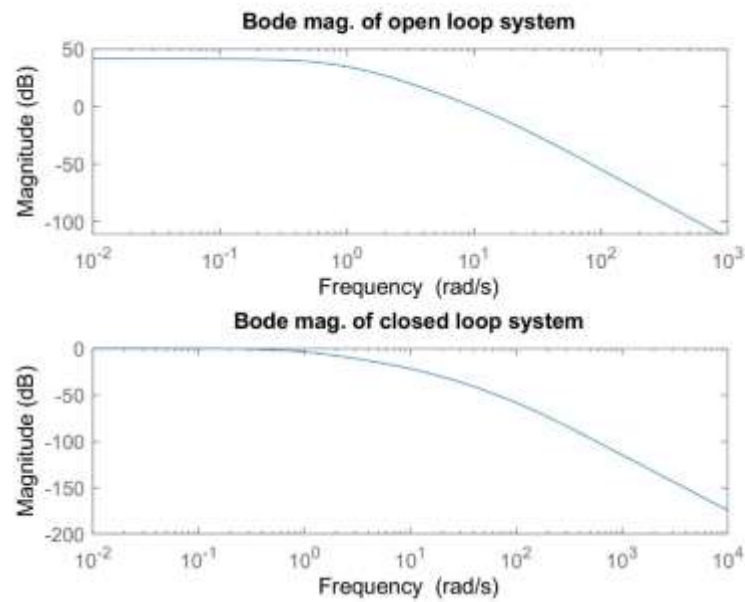
**Fig. 84:** Mu plot of closed system with parametric controller

**Scenario 1:**  $KF=116.8$  ,  $TA=0.06$  ,  $TE=0.7$  ,  $TG=1.5$



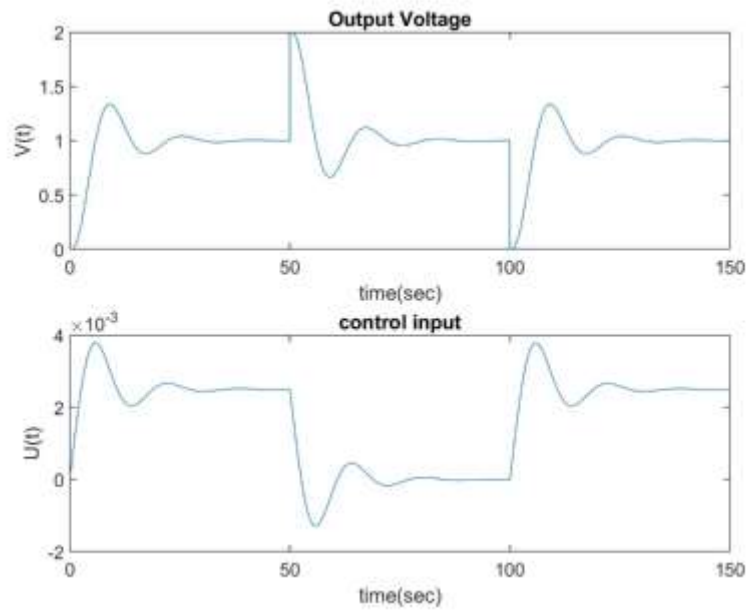
**Fig. 85:** Output voltage and control input for scenario 1

Fig. 85 depicts step response of closed loop system. Fig. 86 depicts bode magnitude diagrams of open loop and closed loop systems.



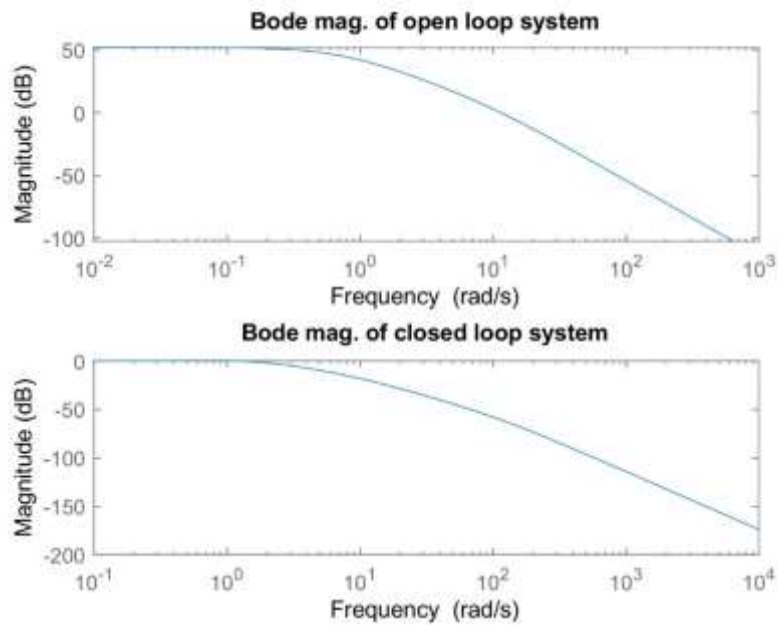
**Fig. 86:** Bode magnitude diagram of open and closed loop systems

**Scenario 2:**  $KF=400$  ,  $TA=0.1$  ,  $TE=1$  ,  $TG=2$



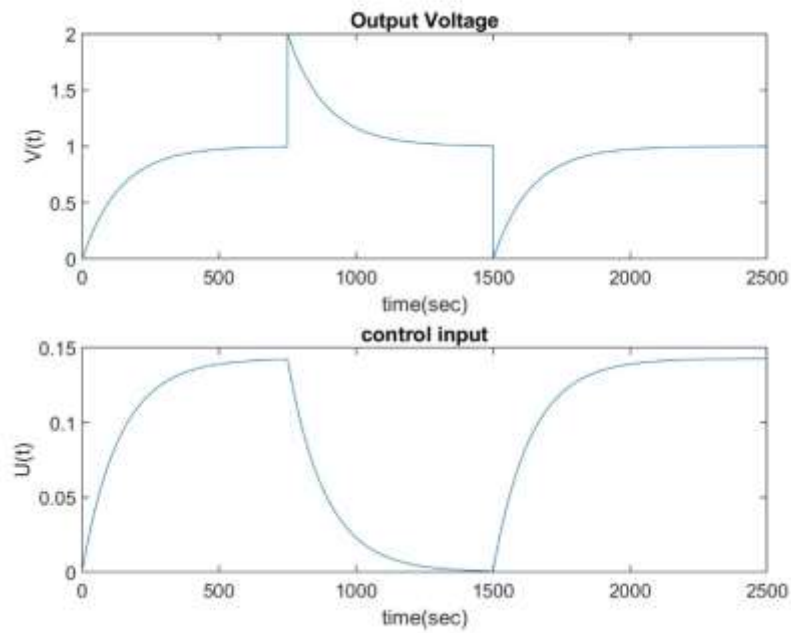
**Fig 87:** Output voltage and control input for scenario 2

Fig. 87 depicts step response of closed loop system. Fig. 88 depicts bode magnitude diagrams of open loop and closed loop systems.



**Fig. 88:** Bode magnitude diagram of open and closed loop systems

**Scenario 3:**  $KF=7$  ,  $TA=0.02$  ,  $TE=0.4$  ,  $TG=1$



**Fig. 89:** Output voltage and control input for scenario 3

Fig. 89 depicts step response of closed loop system. Fig. 90 depicts bode magnitude diagrams of open loop and closed loop systems.

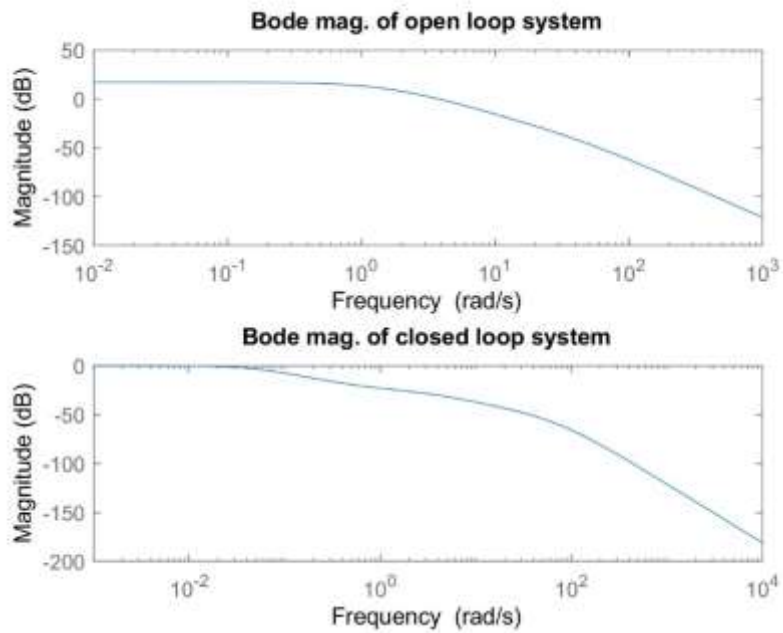


**Fig. 90:** Bode magnitude diagram of open and closed loop systems

## Simulation a real synchronous generator connected to a 230 kV network

Fig. 91 and 92 represent the deviation of the voltage by the parametric controller.

**Scenario 1:**  $K_A=40$  ,  $K_E=10$  (maximum)

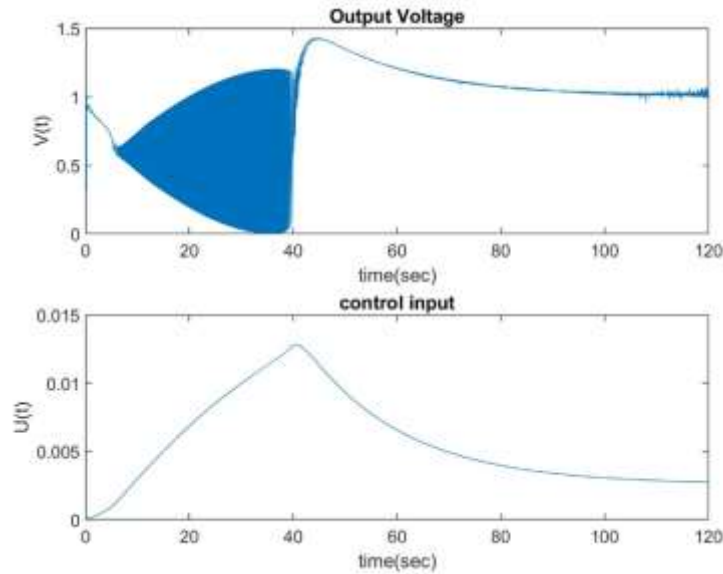


**Fig. 91:** Terminal voltage and control input for scenario 1

**Scenario 2:**  $K_A=10$  ,  $K_E=1$  (minimum)

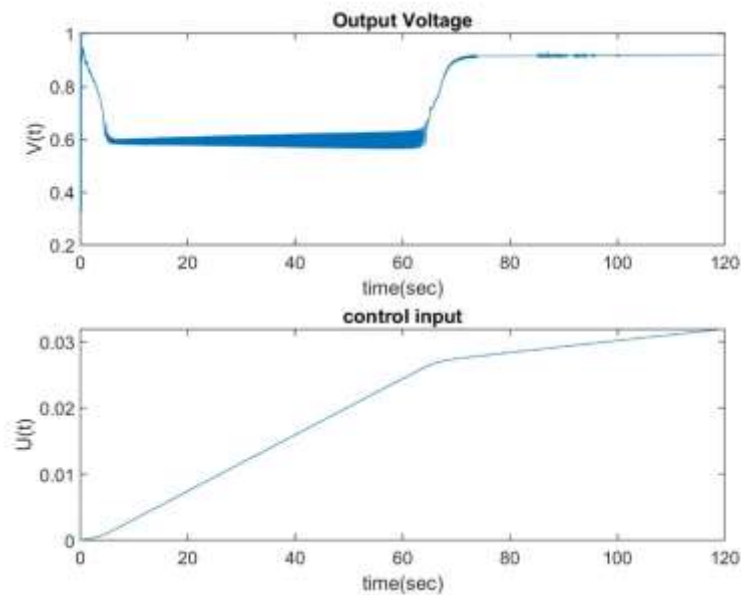


**Fig. 92:** Terminal voltage and control input for scenario 2

## Conclusion

In this research work,  $\mu$ -synthesis,  $H_\infty$ (RICC & LMI),  $H_2$ ,  $H_2/H_\infty$  and parameteric control design methods have been used to set the synchronous generator's terminal voltage. By defining a new gain coefficient as AVR gain which is equal to the multiplication of the gain coefficients of the exciter, the amplifier and the generator, the system has four real structured parameters. The large deviations and the four real structured uncertainties cause the design procedures to be complicated. The above mentioned controllers have been designed to decrease the impacts of generator output disturbance and reference voltage tracking. The table below compares these five designed controllers together plus the controller designed in reference paper[1].

**Table 2**

	<b>Controller order</b>	<b><math>\mu</math> (robust perf.)</b>	<b>Steady state error(nominal)</b>	<b>Settling time(nominal)</b>
<b>Ref. paper</b>	6	$< 1$	0	1
<b><math>\mu</math>-synthesis</b>	7	$< 1$	0	11
<b><math>H_\infty</math>-ricc</b>	15	$< 1$	0	35
<b><math>H_\infty</math>-lmi</b>	15	$< 1$	0	43
<b><math>H_2</math></b>	11	$< 1$	0	42
<b><math>H_2/H_\infty</math></b>	14	$< 1$	2%	106
<b>parameteric</b>	4	$\cong 2.7$	0	19

**Solution:** select multiplicative weighting function fairly realistic and utilize options of software for real uncertainties to avoid more conservations in controller design while calculating  $\mu$  maintain its value less than one and achieve better responses.

## References

- [1] Modabbernia M., Alizadeh B., Saheb A., Mirhosseini Moghaddam M.; Robust Control of Automatic Voltage Regulator (AVR) with Real Structured Parameteric Uncertainties Based on  $H_\infty$  and  $\mu$ -analysis. ISA Transactions 100 (2020) 46-62
- [2] Zou K., Doyle J.C.; Essentials of Robust Control. Prentice Hall; 1999
- [3] Doyle J., Francis B., Tannenbaum A.; Feedback Control Theory. Macmillan Publishing Co.; 1990

## Appendix

In order to watch simulations, the m.files of Code folder could be easily run.

### Section 2

```

clc;
clear
close all

s=tf('s')
G0=(210.5/(0.06*s+1))*(1/(0.7*s+1))*(1/(1.5*s+1));
figure
for KF=7:196.5:400
    for TA=0.02:0.04:0.1
        for TE=0.4:0.3:1
            for TG=1:1:2
                G=(KF/(TA*s+1))*(1/(TE*s+1))*(1/(TG*s+1));
                W=(G/G0)-1;
                bodemag(W)
                hold on
            end
        end
    end
end
hold on
bodemag(15*(s+1)/(s+10), '*r')

```



```

clc
clear
close all

s=tf('s')
%% define weighting matrices
a=1;b=220;c=210000;dd=1;
ee=1;f=1;g=1;h=20;
Ws=(a*s+b)/(c*s+dd);
Wu=(ee*s+f)/(g*s+h);
Ws_1=1/Ws;
omega=logspace(-2,3,200);
figure
bodemag(Ws_1)
legend('1/Wp')
figure
bodemag(Wu,omega)
legend('Wu')
Wn=1/(0.006*s+1);

%% constructing interconnected system for uncertain plant
G0=(203.5/(0.06*s+1))*(1/(0.7*s+1))*(1/(1.5*s+1));
delta=ultidyn('delta',[1 1]);
W=10*(s+1)/(s+10);
G=G0*(1+W*delta);
M=iconnect;
r=icsignal(1);
d=icsignal(1);
n=icsignal(1);
e=icsignal(1);
u=icsignal(1);
zs=icsignal(1);
zu=icsignal(1);
M.Equation{1}=equate(e,r-Wn*(n+d+G*u));
M.Input=[r;d;n;u];
M.Output=[Ws*e;Wu*u;e];
T=tf(M.System)

%% designing controller by mu-synthesis method
[k,c1,bnd,dkinf]=dksyn(M.System,1,1)
tf(k)
zpk(k)
figure
bodemag(k)
legend('K')
title('Bode mag. of Mu-synthesis controller')

```

```
%% reference input step response
```

Move here to reveal tool

```
G1=(203.5/(0.06*s+1))*(1/(0.7*s+1))*(1/(1.5*s+1));
GG=k*G1/(1+G1*k*Wn);
figure
step(G1)
title('step response of open loop sys.')
figure
step(GG)
title('step response of closed loop sys.')
figure
subplot(2,1,1)
bodemag(G1)
title('Bode mag. of open loop sys.')
subplot(2,1,2)
bodemag(GG)
title('Bode mag. of closed loop sys.')
```

```
%% mu-plot of each iteration
```

```
figure
l1=semilogx(dkinf{1,1}.MussvBnds(:,2),'k--')
hold on
l1.LineWidth=2;
l2=semilogx(dkinf{1,2}.MussvBnds(:,2),'g-')
l2.LineWidth=2;
hold on
l3=semilogx(dkinf{1,3}.MussvBnds(:,2),'r:')
l3.LineWidth=2;
legend('\mu_1', '\mu_2', '\mu_3')
```

```
%% state-space and transfer function representation of interconnected sys.
```

```
TA=0.06;TE=0.7;TG=1.5;KS=1;TS=0.006;PTA=0.67;PTE=0.43;PTG=1/3;KF=203.5;PKF=0.966;
z1=a/c;z2=(b/dd)-(a/c);z3=c/dd;x1=ee/g;x2=(f/h)-(ee/g);x3=g/h;
A=[-1/TA 0 0 0 0
    1/TE -1/TE 0 0 0
    0 1/TG -1/TG 0 0
    0 0 KS/TS -1/TS 0
    0 0 0 -z2/z3 -1/z3
    0 0 0 0 -1/x3];
B1=[1/TA -PTA/TA 0 0 0
    0 0 -PTE/TE 0 0
    0 0 0 -PTG/TE 0
    0 0 0 0 KS/TS KS/TS
    0 0 0 0 z2/z3 0
    0 0 0 0 0 0];
```

```

C1=[0 0 0 0 0 0
    -1 0 0 0 0 0
    1 -1 0 0 0 0
    0 1 -1 0 0 0
    0 0 0 -z1 1 0
    0 0 0 0 0 1];
B2=[KF/TA;0;0;0;0;x2/x3];
C2=[0 0 0 -1 0 0];
D11=[0 0 0 0 0 0
    1 -PTA 0 0 0 0
    0 0 -PTE 0 0 0
    0 0 0 -PTG 0 0 0
    0 0 0 0 z1 0
    0 0 0 0 0 0];
D12=[KF*PKF;KF;0;0;0;x1];
D21=[0 0 0 0 1 0 0];
D22=[0];
B=[B1 B2];
C=[C1;C2];
D=[D11 D12;D21 D22];
M2=C*inv(s*eye(6)-A)*B+D;
M11=M2(1:6,1:7);
M12=M2(1:6,8);
M21=M2(7,1:7);
M22=M2(7,8);

%% lower LFT ( F_l(M,K) )
Tzw=M11+M12*k*inv(eye(1)-M22*k)*M21;

%% mu-plot (obtained final mu)
block=[1 0;1 0;1 0;1 0;3 2];
[bounds,muinfo]=mussv(Tzw,block);
bounds
figure
semilogx(bounds(:,2))
axis([0.00001 10000 0 3])

%% time responses
figure
subplot(2,1,1)
simout=sim('AVR_Mu_synthesis__')
plot(simout.v(:,1))
xlabel('time(sec)');ylabel('V(t)')
title('Output Voltage')

hold on
subplot(2,1,2)
plot(simout.u(:,1))
xlabel('time(sec)');ylabel('U(t)')
title('control input')

```

[Move here to](#)

## Section 3

```

s=tf('s')
%% define weighting matrices
a=1;b=0.2;c=1400;d=1.2;
e=0.1;f=3;g=0.1;h=2.3;
Ws=(a*s+b)/(c*s+d);
Wu=(e*s+f)/(g*s+h);
Ws_1=1/Ws;
figure
bodemag(Ws_1)
legend('1/Wp')
title('Bode mag. diagram of 1/Wp')
figure
bodemag(Wu)
legend('Wu')
title('Bode mag.diagram of Wu')

%% interconnected system for nominal plant
Wn=1/(0.0305*s+1);
G0=(116.8/(0.06*s+1))*(1/(0.7*s+1))*(1/(1.5*s+1));
systemnames='G0 Ws Wu Wn';
inputvar='[r;d;n;u]';
outputvar='[Ws;Wu;r-Wn]';
input_to_G0='[u]';
input_to_Ws='[r-Wn]';
input_to_Wn='[n+G0]';
input_to_Wu='[u]';
sysoutname='P_ic';
cleanupsysic='yes';
sysic
P_ic=minreal(P_ic);

%% design H-inf controller
[k,cl,gg,info]=hinfsyn(P_ic,1,1);
tf(k)
zpk(k)
% figure
% sigma(cl)
% title('Singular values of closed loop system')
k1=k*(s+0.0008571)/s;
tf(k1)

```

```

figure
bodemag(k1)
title('Bode mag. of H-inf controller')
c11=P_ic(1:2,1:3)+P_ic(1:2,4)*k1*inv(1-P_ic(3,4)*k1)*P_ic(3,1:3);
c11.D=[];
tf(c11);
zpk(c11);
figure
sigma(c11)
title('Singular values of closed loop system')

%% reference input step response
Wn_1=1/(0.006*s+1);
G1=(116.8/(0.06*s+1))*(1/(0.7*s+1))*(1/(1.5*s+1));
GG=k1*G1/(1+G1*k1*Wn_1);
figure
step(G1)
title('Step response of open loop sys.')
figure
step(GG)
title('Step response of closed loop sys.')
figure
subplot(2,1,1)
bodemag(G1)
title('Bode mag. of open loop sys.')
subplot(2,1,2)
bodemag(GG)
title('Bode mag. of closed loop sys.')

%% stste space and transfer function representation of interconnected sys.
TA=0.06;TE=0.7;TG=1.5;KS=1;TS=0.006;PTA=0.67;PTE=0.43;PTG=1/3;KF=203.5;PKF=0.966;
z1=a/c;z2=(b/d)-(a/c);z3=c/d;x1=e/g;x2=(f/h)-(e/g);x3=g/h;
A=[-1/TA 0 0 0 0 0
    1/TE -1/TE 0 0 0 0
    0 1/TG -1/TG 0 0 0
    0 0 KS/TS -1/TS 0 0
    0 0 0 -z2/z3 -1/z3 0
    0 0 0 0 0 -1/x3];
B1=[1/TA -PTA/TA 0 0 0 0
    0 0 -PTE/TE 0 0 0
    0 0 0 -PTG/TE 0 0
    0 0 0 0 KS/TS KS/TS
    0 0 0 0 z2/z3 0
    0 0 0 0 0 0];

```



```

C1=[0 0 0 0 0 0
    -1 0 0 0 0 0
    1 -1 0 0 0 0
    0 1 -1 0 0 0
    0 0 0 -z1 1 0
    0 0 0 0 0 1];
B2=[KF/TA;0;0;0;0;x2/x3];
C2=[0 0 0 -1 0 0];
D11=[0 0 0 0 0 0
    1 -PTA 0 0 0 0
    0 0 -PTE 0 0 0
    0 0 0 -PTG 0 0 0
    0 0 0 0 z1 0 0
    0 0 0 0 0 0 0];
D12=[KF*PKF;KF;0;0;0;x1];
D21=[0 0 0 0 1 0 0];
D22=[0];
B=[B1 B2];
C=[C1;C2];
D=[D11 D12;D21 D22];
M2=C*inv(s*eye(6)-A)*B+D;
M11=M2(1:6,1:7);
M12=M2(1:6,8);
M21=M2(7,1:7);
M22=M2(7,8);

%% lower LFT ( F_1(M,K) )
Tzw=M11+M12*k1*inv(eye(1)-M22*k1)*M21;

%% Mu plot (obtained final Mu)
block=[1 0;1 0;1 0;1 0;3 2];
[bounds,muinfo]=mussv(Tzw,block);
figure
semilogx(bounds(:,2))
title('Mu plot of closed loop system with H-inf controller')

%% time responses
figure
subplot(2,1,1)
simout=sim('AVR_H_inf__')
plot(simout.v(:,1))
xlabel('time(sec)');ylabel('V(t)')
title('Output Voltage')

hold on
subplot(2,1,2)
plot(simout.u(:,1))
xlabel('time(sec)');ylabel('U(t)')
title('control input')

```

[Move here to](#)

```

clc
clear
close all

s=tf('s')
%% define weighting matrices
a=5;b=1;c=1100;d=28;
e=0.1;f=4.9;g=1;h=2;
Ws=(a*s+b)/(c*s+d);
Wu=(e*s+f)/(g*s+h);
Ws_1=1/Ws;
figure
bodemag(Ws_1)
legend('1/Wp')
title('Bode mag. diagram of 1/Wp')
figure
bodemag(Wu)
legend('Wu')
title('Bode mag.diagram of Wu')

%% interconnected system for nominal plant
Wn=1/(0.0305*s+1);
G0=(116.8/(0.06*s+1))*(1/(0.7*s+1))*(1/(1.5*s+1));
systemnames='G0 Ws Wu Wn';
inputvar='[r;d;n;u]';
outputvar='[Ws;Wu;r-Wn]';
input_to_G0='[u]';
input_to_Ws='[r-Wn]';
input_to_Wn='[n+G0]';
input_to_Wu='[u]';
sysoutname='P_ic';
cleanupsysic='yes';
sysic
P_ic=minreal(P_ic);

%% design H-inf controller
opts=hinfsvOptions('Method','LMI');
[k,cl,g,info]=hinfsv(P_ic,1,1,opts);
tf(k)
zpk(k)
% figure
% sigma(cl)
% title('Singular values of closed loop system')
k1=k*(s+0.02546)/s;
tf(k1)
figure
bodemag(k1)

```

```

title('Bode mag. of H-inf controller')
c11=P_ic(1:2,1:3)+P_ic(1:2,4)*k1*inv(1-P_ic(3,4)*k1)*P_ic(3,1:3);
c11.D=[];
tf(c11);
zpk(c11);
figure
sigma(c11)
title('Singular values of closed loop system')

%% reference input step response
Wn_1=1/(0.006*s+1);
G1=(116.8/(0.06*s+1))*(1/(0.7*s+1))*(1/(1.5*s+1));
GG=k1*G1/(1+G1*k1*Wn_1);
figure
step(G1)
title('Step response of open loop sys.')
figure
step(GG)
title('Step response of closed loop sys.')
figure
subplot(2,1,1)
bodemag(G1)
title('Bode mag. of open loop sys.')
subplot(2,1,2)
bodemag(GG)
title('Bode mag. of closed loop sys.')

%% stste space and transfer function representation of interconnected sys.
TA=0.06;TE=0.7;TG=1.5;KS=1;TS=0.006;PTA=0.67;PTE=0.43;PTG=1/3;KF=203.5;PKF=0.966;
z1=a/c;z2=(b/d)-(a/c);z3=c/d;x1=e/g;x2=(f/h)-(e/g);x3=g/h;
A=[-1/TA 0 0 0 0 0
    1/TE -1/TE 0 0 0 0
    0 1/TG -1/TG 0 0 0
    0 0 KS/TS -1/TS 0 0
    0 0 0 -z2/z3 -1/z3 0
    0 0 0 0 -1/x3];
B1=[1/TA -PTA/TA 0 0 0 0 0
    0 0 -PTE/TE 0 0 0 0
    0 0 0 -PTG/TE 0 0 0
    0 0 0 0 KS/TS KS/TS
    0 0 0 0 z2/z3 0 0
    0 0 0 0 0 0 0];

```



```

C1=[0 0 0 0 0 0
    -1 0 0 0 0 0
    1 -1 0 0 0 0
    0 1 -1 0 0 0
    0 0 0 -z1 1 0
    0 0 0 0 0 1];
B2=[KF/TA;0;0;0;0;x2/x3];
C2=[0 0 0 -1 0 0];
D11=[0 0 0 0 0 0
    1 -PTA 0 0 0 0
    0 0 -PTE 0 0 0
    0 0 0 -PTG 0 0 0
    0 0 0 0 z1 0
    0 0 0 0 0 0];
D12=[KF*PKF;KF;0;0;0;x1];
D21=[0 0 0 0 1 0 0];
D22=[0];
B=[B1 B2];
C=[C1;C2];
D=[D11 D12;D21 D22];
M2=C*inv(s*eye(6)-A)*B+D;
M11=M2(1:6,1:7);
M12=M2(1:6,8);
M21=M2(7,1:7);
M22=M2(7,8);

%% lower LFT ( F_l(M,K) )
Tzw=M11+M12*k1*inv(eye(1)-M22*k1)*M21;

%% Mu plot (obtained final Mu)
block=[1 0;1 0;1 0;1 0;3 2];
[bounds,muinfo]=mussv(Tzw,block);
bounds
figure
semilogx(bounds(:,2))
title('Mu plot of closed loop system with H-inf(LMI) controller')

%% time responses
figure
subplot(2,1,1)
simout=sim('AVR_H_inf_LMI__')
plot(simout.v(:,1))
xlabel('time(sec)');ylabel('V(t)')
title('Output Voltage')

hold on
subplot(2,1,2)
plot(simout.u(:,1))
xlabel('time(sec)');ylabel('U(t)')
title('control input')

```

Move here to

## Section 4

```

clc
clear
close all

s=tf('s')
%% define weighting matrices
a=1;b=18;c=10;d=100;
e=1;f=280;g=80;h=100;
Ws=(a*s+b)/(c*s+d);
Wu=(e*s+f)/(g*s+h);
Ws_1=1/Ws;
figure
bodemag(Ws_1)
legend('1/Wp')
title('Bode mag. diagram of 1/Wp')
figure
bodemag(Wu)
legend('Wu')
title('Bode mag.diagram of Wu')

%% interconnected system for nominal plant
Wn=1/(0.0305*s+1);
G0=(116.8/(0.06*s+1))*(1/(0.7*s+1))*(1/(1.5*s+1));
systemnames='G0 Ws Wu Wn';
inputvar='[r;d;n;u]';
outputvar='[Ws;Wu;r-Wn]';
input_to_G0='[u]';
input_to_Ws='[r-Wn]';
input_to_Wn='[n+G0]';
input_to_Wu='[u]';
sysoutname='P_ic';
cleanup_sysic='yes';
sysic
P_ic=minreal(P_ic);

%% design H-inf controller
[k,cl,gg,info]=h2syn(P_ic,1,1);
tf(k)
zpk(k)
%figure
%sigma(cl)
%title('Singular values of closed loop system')
cl.D=[];
norm(cl,2)

```

Move here to

```

%% reduce controller order
k1=modred(k,11:14,'Truncate');
tf(k1)
zpk(k1)
k2=k1*(s+1.243)/s;
tt=tf(k2)
zpk(k2)
figure
bodemag(k2)
title('Bode mag. of H2 controller')
c11=P_ic(1:2,1:3)+P_ic(1:2,4)*k2*inv(1-P_ic(3,4)*k2)*P_ic(3,1:3);
c11.D=[];
tf(c11)
zpk(c11)
figure
sigma(c11)
title('Singular values of closed loop system')
n=norm(c11,2)

%% reference input step response
Wn_1=1/(0.006*s+1);
G1=(100/(0.06*s+1))*(1/(0.7*s+1))*(1/(1.5*s+1));
GG=k2*G1/(1+G1*k2*Wn_1);
figure
step(G1)
title('Step response of open loop sys.')
figure
step(GG)
title('Step response of closed loop sys.')
figure
subplot(2,1,1)
bodemag(G1)
title('Bode mag. of open loop sys.')
subplot(2,1,2)
bodemag(GG)
title('Bode mag. of closed loop sys.')

%% stste space and transfer function representation of interconnected sys.
TA=0.06;TE=0.7;TG=1.5;KS=1;TS=0.006;PTA=0.67;PTE=0.43;PTG=1/3;KF=203.5;PKF=0.966;
z1=a/c;z2=(b/d)-(a/c);z3=c/d;x1=e/g;x2=(f/h)-(e/g);x3=g/h;
A=[-1/TA 0 0 0 0
    1/TE -1/TE 0 0 0
    0 1/TG -1/TG 0 0
    0 0 KS/TS -1/TS 0
    0 0 0 -z2/z3 -1/z3
    0 0 0 0 -1/x3];

```

```

B1=[1/TA -PTA/TA 0 0 0 0 0
     0 0 -PTE/TE 0 0 0 0
     0 0 0 -PTG/TE 0 0 0
     0 0 0 0 0 KS/TS KS/TS
     0 0 0 0 0 z2/z3 0 0
     0 0 0 0 0 0 0];
C1=[0 0 0 0 0 0
     -1 0 0 0 0 0
     1 -1 0 0 0 0
     0 1 -1 0 0 0
     0 0 0 -z1 1 0
     0 0 0 0 0 1];
B2=[KF/TA;0;0;0;0;x2/x3];
C2=[0 0 0 -1 0 0];
D11=[0 0 0 0 0 0
      1 -PTA 0 0 0 0
      0 0 -PTE 0 0 0
      0 0 0 -PTG 0 0
      0 0 0 0 z1 0
      0 0 0 0 0 0];
D12=[KF*PKF;KF;0;0;0;x1];
D21=[0 0 0 0 1 0];
D22=[0];
B=[B1 B2];
C=[C1;C2];
D=[D11 D12;D21 D22];
M2=C*inv(s*eye(6)-A)*B+D;
M11=M2(1:6,1:7);
M12=M2(1:6,8);
M21=M2(7,1:7);
M22=M2(7,8);

%% lower LFT ( F_l(M,K) )
Tzw=M11+M12*k2*inv(eye(1)-M22*k2)*M21;

%% Mu plot (obtained final Mu)
block=[1 0;1 0;1 0;1 0;3 2];
[bounds,muinfo]=mussv(Tzw,block);
bounds
figure
semilogx(bounds(:,2))
title('Mu plot of closed loop system with H2 controller')
hold on
subplot(2,1,2)
plot(simout.u(:,1))
xlabel('time(sec)');ylabel('U(t)')
title('control input')

```

[Move here to](#)

## Section 5

```

clc
clear
close all

s=tf('s')
%% define weighting matrices
a=1;b=0.3;c=500;d=0.3;
e=1;f=4.5;g=3;h=2.8;
Ws=(a*s+b)/(c*s+d);
Wu=(e*s+f)/(g*s+h);
Ws_1=1/Ws;
figure
bodemag(Ws_1)
legend('1/Wp')
title('Bode mag. diagram of 1/Wp')
figure
bodemag(Wu)
legend('Wu')
title('Bode mag.diagram of Wu')

%% interconnected system for nominal plant
Wn=1/(0.0305*s+1);
G0=(116.8/(0.06*s+1))*(1/(0.7*s+1))*(1/(1.5*s+1));
systemnames='G0 Ws Wu Wn';
inputvar='[r;d;n;u]';
outputvar='[Ws;Wu;r-Wn]';
input_to_G0='[u]';
input_to_Ws='[r-Wn]';
input_to_Wn='[n+G0]';
input_to_Wu='[u]';
sysoutname='P_ic';
cleanupysic='yes';
sysic
P_ic=minreal(P_ic);

%% design H-inf controller
wz=[1 1];
[k,cl,gg,info]=h2hinfsyn(ss(P_ic),1,1,1,wz);
tf(k)
zpk(k)
figure
sigma(cl)
title('Singular values of closed loop system')
figure
bodemag(k)
title('Bode mag. of H2/Hinf controller')

```

Move here to

```
%% reference input step response
```

[Move here to reveal tools](#)

```
Wn_1=1/(0.006*s+1);
G1=(116.8/(0.06*s+1))*(1/(0.7*s+1))*(1/(1.5*s+1));
GG=k*G1/(1+G1*k*Wn_1);
figure
step(G1)
title('Step response of open loop sys.')
figure
step(GG)
title('Step response of closed loop sys.')
figure
subplot(2,1,1)
bodemag(G1)
title('Bode mag. of open loop sys.')
subplot(2,1,2)
bodemag(GG)
title('Bode mag. of closed loop sys.')
```

```
%% stste space and transfer function representation of interconnected sys.
```

```
TA=0.06;TE=0.7;TG=1.5;KS=1;TS=0.006;PTA=0.67;PTE=0.43;PTG=1/3;KF=203.5;PKF=0.966;
z1=a/c;z2=(b/d)-(a/c);z3=c/d;x1=e/g;x2=(f/h)-(e/g);x3=g/h;
A=[-1/TA 0 0 0 0 0
    1/TE -1/TE 0 0 0 0
    0 1/TG -1/TG 0 0 0
    0 0 KS/TS -1/TS 0 0
    0 0 0 -z2/z3 -1/z3 0
    0 0 0 0 0 -1/x3];
B1=[1/TA -PTA/TA 0 0 0 0 0
    0 0 -PTE/TE 0 0 0 0
    0 0 0 -PTG/TE 0 0 0
    0 0 0 0 0 KS/TS KS/TS
    0 0 0 0 z2/z3 0 0
    0 0 0 0 0 0 0];
C1=[0 0 0 0 0 0
    -1 0 0 0 0 0
    1 -1 0 0 0 0
    0 1 -1 0 0 0
    0 0 0 -z1 1 0
    0 0 0 0 0 1];
B2=[KF/TA;0;0;0;0;x2/x3];
C2=[0 0 0 -1 0 0];
```



```

D11=[0 0 0 0 0 0 0
      1 -PTA 0 0 0 0 0
      0 0 -PTE 0 0 0 0
      0 0 0 -PTG 0 0 0
      0 0 0 0 z1 0 0
      0 0 0 0 0 0 0];
D12=[KF*PKF;KF;0;0;0;x1];
D21=[0 0 0 0 1 0 0];
D22=[0];
B=[B1 B2];
C=[C1;C2];
D=[D11 D12;D21 D22];
M2=C*inv(s*eye(6)-A)*B+D;
M11=M2(1:6,1:7);
M12=M2(1:6,8);
M21=M2(7,1:7);
M22=M2(7,8);

%% lower LFT ( F_1(M,K) )
Tzw=M11+M12*k*inv(eye(1)-M22*k)*M21;

%% Mu plot (obtained final Mu)
block=[1 0;1 0;1 0;1 0;3 2];
[bounds,muinfo]=mussv(Tzw,block);
bounds
figure
semilogx(bounds(:,2))
title('Mu plot of closed loop system with H2/Hinf controller')

%% time responses
figure
subplot(2,1,1)
simout=sim('AVR_H2_Hinf__')
plot(simout.v(:,1))
xlabel('time(sec)');ylabel('V(t)')
title('Output Voltage')
hold on
subplot(2,1,2)
plot(simout.u(:,1))
xlabel('time(sec)');ylabel('U(t)')
title('control input')

```

## Section 6

```

clc
clear
close all

s=tf('s')

%% parameteric controller
k=(0.063*s^4+1.245*s^3+3.442*s^2+3.26*s+1)/(0.063*s^4+8.54*s^3+140.3*s^2+148.2*s);
k1=tf(k)
omega=logspace(-3,4,200);
k2=frd(k1,omega);

%% bode mag. of controller and system
G=116.8/((0.06*s+1)*(0.7*s+1)*(1.5*s+1));
Wn=1/(0.006*s+1);
Wn_1=1/Wn;
f=G*k/(1+G*k*Wn_1);
figure
bodemag(k)
title('Bode mag. of parameteric controller')
figure
subplot(2,1,1)
bodemag(G)
title('Bode mag. of open loop system')
subplot(2,1,2)
bodemag(f)
title('Bode mag. of closed loop system')

%% stste space and transfer function representation of interconnected sys.
a=1;b=1;c=1;d=1;e=1;f=1;g=1;h=1;
TA=0.06;TE=0.7;TG=1.5;KS=1;TS=0.006;PTA=0.67;PTE=0.43;PTG=1/3;KF=203.5;PKF=0.966;
z1=a/c;z2=(b/d)-(a/c);z3=c/d;x1=e/g;x2=(f/h)-(e/g);x3=g/h;
A=[-1/TA 0 0 0 0 0
    1/TE -1/TE 0 0 0 0
    0 1/TG -1/TG 0 0 0
    0 0 KS/TS -1/TS 0 0
    0 0 0 -z2/z3 -1/z3 0
    0 0 0 0 0 -1/x3];
B1=[1/TA -PTA/TA 0 0 0 0 0
    0 0 -PTE/TE 0 0 0 0
    0 0 0 -PTG/TE 0 0 0
    0 0 0 0 0 KS/TS KS/TS
    0 0 0 0 z2/z3 0 0
    0 0 0 0 0 0 0];

```



```

C1=[0 0 0 0 0 0
    -1 0 0 0 0 0
    1 -1 0 0 0 0
    0 1 -1 0 0 0
    0 0 0 -z1 1 0
    0 0 0 0 0 1];
B2=[KF/TA;0;0;0;0;x2/x3];
C2=[0 0 0 -1 0 0];
D11=[0 0 0 0 0 0
     1 -PTA 0 0 0 0
     0 0 -PTE 0 0 0
     0 0 0 -PTG 0 0 0
     0 0 0 0 z1 0 0
     0 0 0 0 0 0];
D12=[KF*PKF;KF;0;0;0;x1];
D21=[0 0 0 0 1 0 0];
D22=[0];
B=[B1 B2];
C=[C1;C2];
D=[D11 D12;D21 D22];
M2=C*inv(s*eye(6)-A)*B+D;
M11=M2(1:6,1:7);
M12=M2(1:6,8);
M21=M2(7,1:7);
M22=M2(7,8);

%% lower LFT ( F_l(M,K) )
Tzw=M11+M12*k2*inv(eye(1)-M22*k2)*M21;

%% Mu plot (obtained final Mu)
block=[1 0;1 0;1 0;1 0;3 2];
[bounds,muinfo]=mussv(Tzw,block);
bounds
figure
semilogx(bounds(:,2))
title('Mu plot of closed loop system with parameteric controller')

%% time responses
figure
subplot(2,1,1)
simout=sim('AVR_parameteric__')
plot(simout.v(:,1))
xlabel('time(sec)');ylabel('V(t)')
title('Output Voltage')
hold on
subplot(2,1,2)
plot(simout.u(:,1))
xlabel('time(sec)');ylabel('U(t)')
title('control input')

```

Move here to